AD-A111 820 DAVID W TAYLOR NAVAL SHIP RESEARCH AND DEVELOPMENT CE--ETC F/G 20/1
COMPUTATION OF STEADY-STATE SCATTERED SOUND FROM SUBMERGED INFI--ETC(U)
FEB 82 F M HENDERSON

UNCLASSIFIED DTNSRDC-82/012 NL

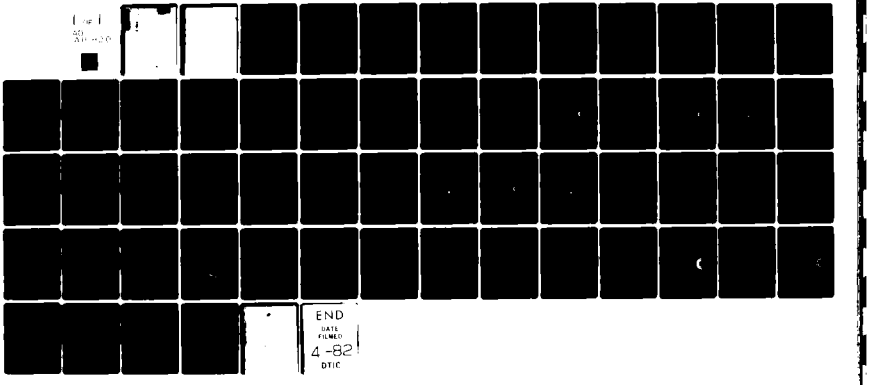

END
DATE FILMED
4-82
DTIC

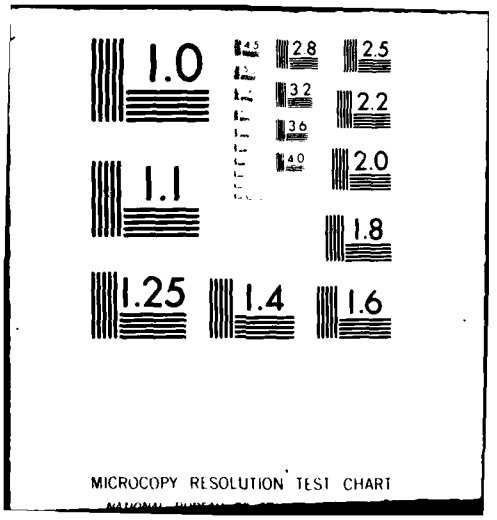
1.0
1.1
1.25
1.4
1.6
1.8
2.0
2.2
2.5
2.8
3.2
3.6
4.0
MICROCOPY RESOLUTION TEST CHART

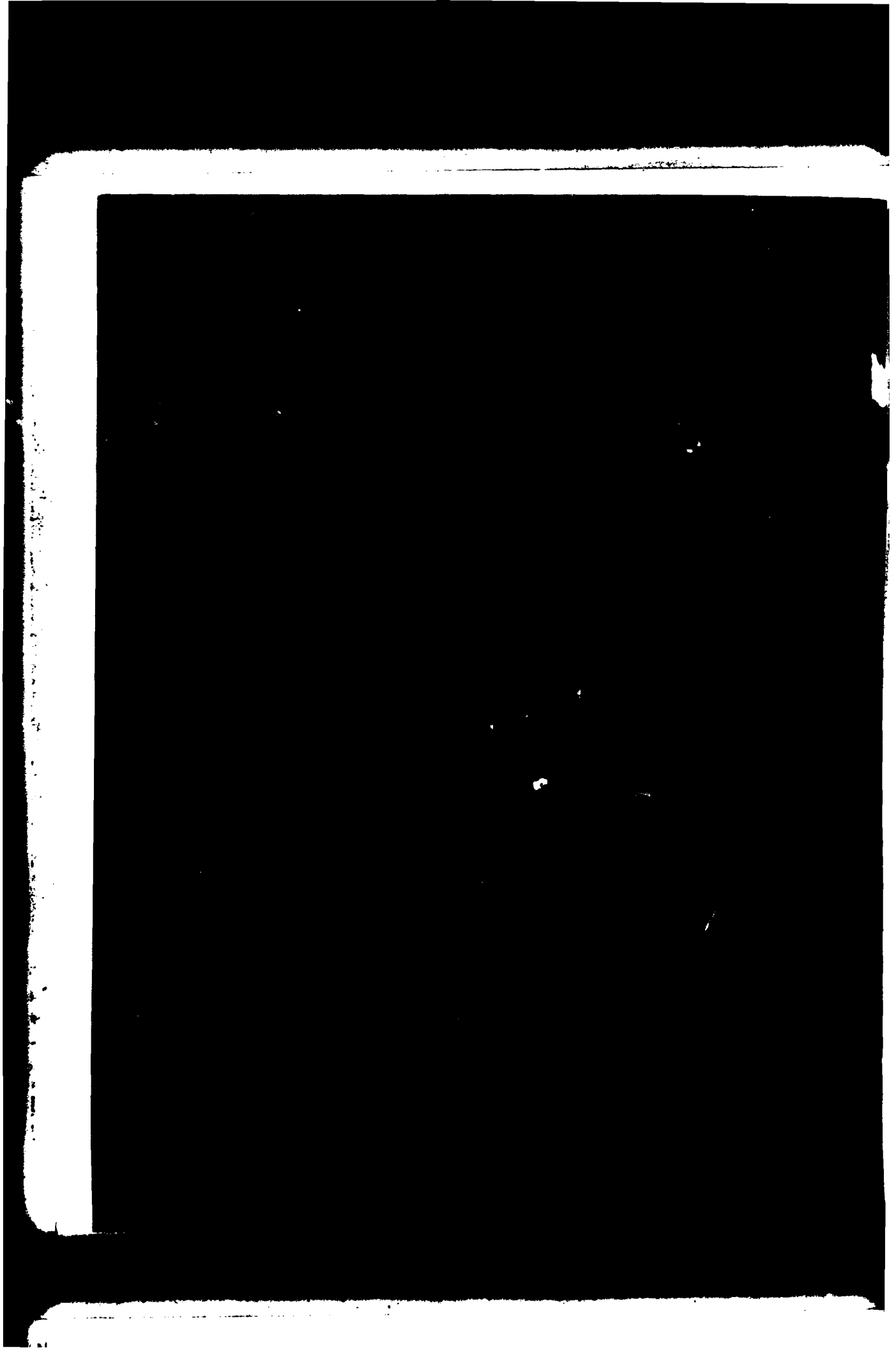

UNCLASSIFIED

SECURITY CLASSIFICATION OF THIS PAGE (When Data Entered)

REPORT DOCUMENTATION PAGE		READ INSTRUCTIONS BEFORE COMPLETING FORM
1. REPORT NUMBER DTNSRDC-82/012	2. GOVT ACCESSION NO.	3. RECIPIENT'S CATALOG NUMBER
4. TITLE (and Subtitle) COMPUTATION OF STEADY-STATE SCATTERED SOUND FROM SUBMERGED INFINITE CYLINDERS BY A STRUCTURAL ANALOG METHOD		5. TYPE OF REPORT & PERIOD COVERED 6. PERFORMING ORG. REPORT NUMBER
7. AUTHOR(s) Francis M. Henderson		8. CONTRACT OR GRANT NUMBER(s)
9. PERFORMING ORGANIZATION NAME AND ADDRESS David W. Taylor Naval Ship Research and Development Center Bethesda, Maryland 20084		10. PROGRAM ELEMENT, PROJECT, TASK AREA & WORK UNIT NUMBERS (See reverse side)
11. CONTROLLING OFFICE NAME AND ADDRESS		12. REPORT DATE February 1982 13. NUMBER OF PAGES 53
14. MONITORING AGENCY NAME & ADDRESS(if different from Controlling Office) Naval Sea Systems Command (05H) Washington, D.C. 20360		15. SECURITY CLASS. (of this report) UNCLASSIFIED 15a. DECLASSIFICATION/DOWNGRADING SCHEDULE

16. DISTRIBUTION STATEMENT (of this Report)

APPROVED FOR PUBLIC RELEASE: DISTRIBUTION UNLIMITED

17. DISTRIBUTION STATEMENT (of the abstract entered in Block 20, if different from Report)

18. SUPPLEMENTARY NOTES

19. KEY WORDS (Continue on reverse side if necessary and identify by block number)

Structural Analogies
Symmetric Potential Formulation
Finite Element
Acoustics
Sound Radiation
Sound Scattering
Wave Equation
Wave Absorbing Boundaries

20. ABSTRACT (Continue on reverse side if necessary and identify by block number)

Finite-element formulations of fluid-structure interaction problems based on the use of structural analogies have been used in a wide variety of applications. The formulations originate from analogies that can be derived between the equations of dynamic elastic motion and generalized forms of the scalar wave equation. The analogies prescribe that the fluid can be modeled with structural finite elements to which special material

(Continued on reverse side)

DD FORM 1 JAN 73 1473 EDITION OF 1 NOV 65 IS OBSOLETE
S/N 0102-LF-014-6601

UNCLASSIFIED

SECURITY CLASSIFICATION OF THIS PAGE (When Data Entered)

(Block 10)

SF43400391, Task 23556
Work Unit 1940-020
SR0140301 Task 15321
Work Unit 1808-010

(Block 20 continued)

properties have been assigned. A particular advantage of this approach is the requirement for only a single degree-of-freedom at each field grid point to represent the scalar field variable. In this report the analog formulations are extended to steady-state plane wave scattering by infinite cylinders. Details of implementation of the formulations via the NASTRAN computer program are presented along with calculations of acoustic pressure scattered by submerged rigid cylinders, empty elastic cylinders, and elastic cylinders containing fluids bounded by interior cylinders which may be eccentric with respect to the outer cylinder. Comparison of numerical and analytic results for the rigid and empty elastic cases shows excellent agreement.

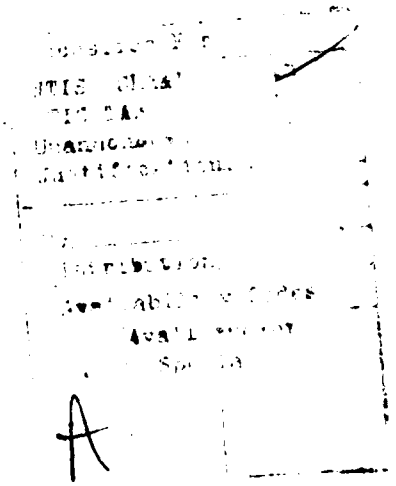

TABLE OF CONTENTS

LIST OF FIGURES

ABSTRACT

Finite-element formulations of fluid-structure interaction problems based on the use of structural analogies have been used in a wide variety of applications. The formulations originate from analogies that can be derived between the equations of dynamic elastic motion and generalized forms of the scalar wave equation. The analogies prescribe that the fluid can be modeled with structural finite elements to which special material properties have been assigned. A particular advantage of this approach is the requirement for only a single degree-of-freedom at each field grid point to represent the scalar field variable. In this report the analog formulations are extended to steady-state plane wave scattering by infinite cylinders. Details of implementation of the formulations via the NASTRAN computer program are presented along with calculations of acoustic pressure scattered by submerged rigid cylinders, empty elastic cylinders, and elastic cylinders containing fluids bounded by interior cylinders which may be eccentric with respect to the outer cylinder. Comparison of numerical and analytic results for the rigid and empty elastic cases shows excellent agreement.

ADMINISTRATIVE INFORMATION

The work presented in this report was conducted with funding from Naval Sea Systems Command (03R11) under Task Area SF43400391, Task 23556, Work Unit 1940-020 and from Naval Sea Systems Command (05H) under Task Area SR0140301, Task 15321, and Work Unit 1808-010.

INTRODUCTION

It is well known that equations which govern the dynamics of various phenomena can in certain instances be brought into identical form with one another to yield an analogy. In the simplest cases, development of the analogy requires merely the identification of correspondences between variables and parameters of the particular equations. A textbook example[1*] of such an analogy is that which exists between the equation of motion for a mass-spring-damper system, Figure 1a

$$\frac{w}{g}\ddot{y} + c\dot{y} + ky = F_o \cos \omega t \qquad (1)$$

*A complete listing of references is given on page 51.

and the equation for current flow in a series-electrical circuit, Figure 1b,

$$L\ddot{I} + R\dot{I} + \frac{1}{C} I = - E_o \sin \omega t \qquad (2)$$

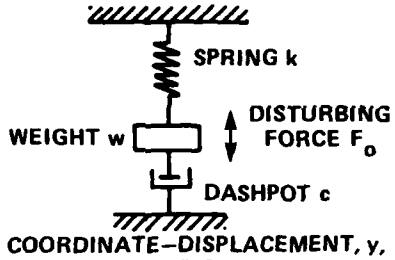

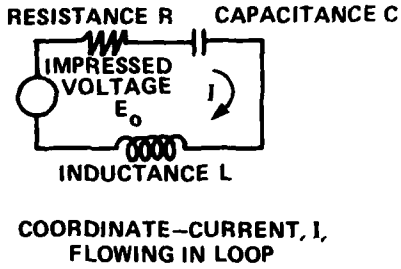

Figure 1a - Mass-Spring-Damper System Figure 1b - Series-Electrical Circuit

Figure 1 - One-Degree-of-Freedom Mechanical and Electrical Systems

These equations can easily be brought into identical form through the following correspondence of parameters:

$$\frac{w}{g} \longleftrightarrow L$$

$$c \longleftrightarrow R$$

$$k \longleftrightarrow \frac{1}{C}$$

$$F_o \longleftrightarrow -E_o$$

$$y \longleftrightarrow I$$

Somewhat more complex analogies are also well known among the partial differential equations which govern various field phenomena. The word "complex" indicates that considerably more effort is required to obtain the identity of form required for the analogies than was required for the simple systems just illustrated. In a recent paper,[2] G.C. Everstine has given details of the development of such analogies between the equations of elasticity and the common equations of classical

mathematical physics such as the wave equation, Helmholtz's equation, Laplace's equation, Poisson's equation, the heat equation, telegraph equation, etc. Various of these analogies have been used with NASTRAN, a standard general-purpose structural analysis computer code, in such applications as generating fully coupled added mass matrices, natural frequencies of general fluid-structure systems, steady-state forced response of fluid-structure systems, shock response of general fluid-structure systems, free-surface potential flow problems, and torsion of prismatic bars of arbitrary cross section. References for these applications are given in Everstine's paper.[2]

The work reported here is an extension of these applications of analogies to steady-state scattering of plane waves from two-dimensional cylindrical shells submerged in an infinite fluid. The particular analogy of interest is one which can be drawn between the wave equation and the equations of classical linear elasticity which NASTRAN solves. Two distinct versions of the analogy can be obtained: (1) a displacement formulation, and (2) a pressure formulation. The latter formulation was chosen for the present work to take advantage of a comparative reduction by a factor of two in the number of degrees-of-freedom required in the finite-element model of the fluid. This report demonstrates the particular form this analogy takes when applied to steady-state scattering and outlines the details of its implementation for computing scattered pressures from infinite cylinders.

SCATTERING FROM A RIGID CYLINDER

VELOCITY POTENTIAL FORMULATION

The first set of calculations using the structural analog was made for scattered pressure from a rigid infinite cylinder ensonified by a steady-state plane wave front. The physical problem is depicted in Figure 2, which is after a drawing in the text by Junger and Feit.[3]

The analog to be used is based on a velocity potential description of the acoustic field, and the mathematical formulation of the physical problem is shown in Figure 3. The radiation condition at infinity is the familiar one for scattering as well as for radiation: there can only be outward traveling waves.

STRUCTURAL ANALOG FORMULATION

This field problem is described via the analog with elasticity. In the detailed development for the case of two-dimensional elasticity,[2] the analog prescribes that

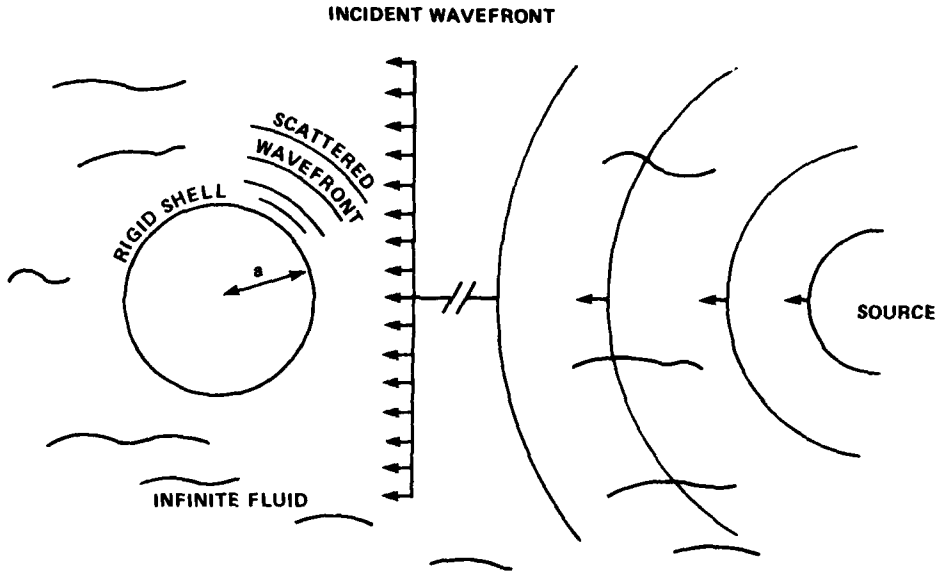

Figure 2 - Rigid Shell Scattering an Incident Plane Wave

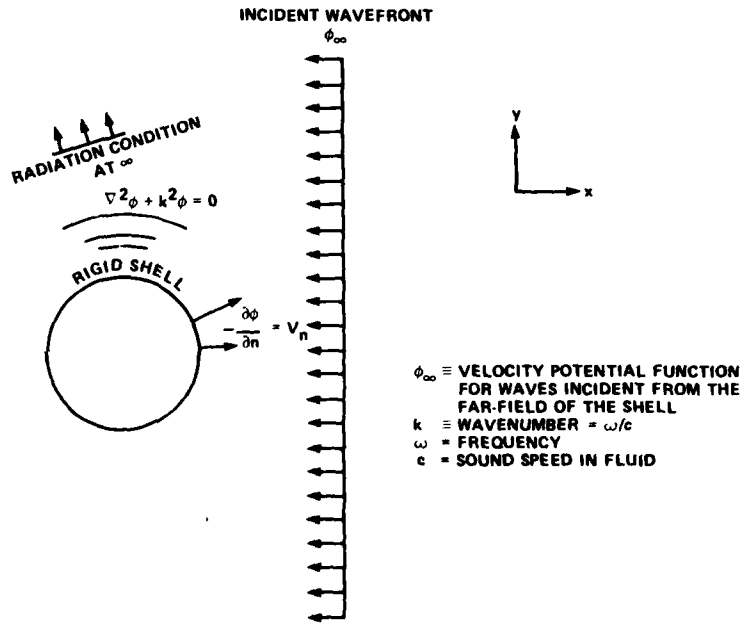

Figure 3 - Velocity Potential Formulation of Field Problem for Scattering

the field be modeled with two-dimensional plane stress finite elements with specially selected mass and elastic properties. These properties are chosen to bring about the necessary identity of form between the equations of elasticity which the structural analysis program solves and the scalar wave equation which governs the scattered field. Either the x- or y-component of displacement may be chosen to correspond to the variable ϕ of the wave equation. Here, it is chosen to be the x-component, giving the correspondence,

$$U_x \longleftrightarrow \phi \tag{3}$$

This states that U_x is the structural analog of the scalar potential ϕ.

The correspondence betweer U_x and ϕ in turn provides the basis for implementing a structural analog of the surface boundary condition as shown in Figure 3. If ϕ can be replaced with U_x, then it is to be expected that the outward normal derivative $\partial\phi/\partial n$ from the fluid can be replaced by $\partial U_x/\partial n$ which has been shown[2] to equal the surface traction divided by the element shear modulus,

$$\frac{\partial U_x}{\partial n} = \frac{T_x^{(n)}}{\mu_e} \tag{4}$$

For a structural surface modeled by finite elements, this expression can be represented[2] by

$$\frac{\partial U_x}{\partial n} = \frac{F_x}{\mu_e A} \tag{5}$$

where F_x is the x-component of the force applied at a grid point on the surface to which area A has been assigned. Comparison of Equation (5) with the surface normal boundary condition (Figure 3) shows that the desired condition is met by setting

$$\frac{F_x}{\mu_e A} = - V_n \tag{6}$$

from which $F_x = -\mu_e A V_n$ is the required load applied at the particular grid point, V_n being the normal velocity outward from the structural surface.

The final part of the analog formulation concerns representation of the radiation condition (Figure 3). One method of treating boundary conditions on an ideally infinite boundary is to represent approximately these conditions on an artifical boundary placed a finite distance from the scattering (or radiating) surface of the structure.

A basis for the analog formulation used here is a boundary condition applied by Zienkiewicz and Newton[4,5] to the artificial bounding surface in radiation problems,

$$\frac{\partial p}{\partial n} = -\frac{1}{c}\frac{\partial p}{\partial t} \tag{7}$$

in which p and t denote acoustic pressure and time, respectively. This expression is strictly valid only for plane waves[4] and hence may be applied at distances from the structural surface at which the outgoing radiating or scattering wave may be reasonably plane, at least in a certain local sense. The relation between acoustic pressure and velocity potential is

$$p = \rho \frac{\partial \phi}{\partial t} \tag{8}$$

where ρ is the fluid density. For time-harmonic ϕ this relation yields

$$p = -i\omega\rho\,\phi \tag{9}$$

which for present purposes may be written

$$p = \alpha\phi \tag{10}$$

with α constant for a given frequency.
Substituting Equation (10) into Equation (7) then gives

$$\alpha \frac{\partial \phi}{\partial n} = -\frac{\alpha}{c}\frac{\partial \phi}{\partial t} \tag{11}$$

or, since $\alpha \neq 0$,

$$\frac{\partial \phi}{\partial n} = -\frac{1}{c}\frac{\partial \phi}{\partial t} \tag{12}$$

According to the analogy of Equation (3), Equation (12) in turn gives

$$\frac{\partial U_x}{\partial n} = -\frac{1}{c}\frac{\partial U_x}{\partial t} \tag{13}$$

Substituting Equation (5) into Equation (13) results in

$$\frac{F_x}{\mu_e A} = -\frac{1}{c}\frac{\partial U_x}{\partial t} \tag{14}$$

or

$$F_x = -\frac{\mu_e A}{c}\frac{\partial U_x}{\partial t} \tag{15}$$

Equation (15) indicates that the analog representation of the condition to be obtained at the assumed finite outer boundary of the exterior fluid (Equation (7)) is achieved through use of scalar dashpots of constant $\mu_e A/c$ connected from the boundary to ground, in agreement with the general form for boundary conditions derived by Everstine.[2] In particular, for the outer boundary modeled by finite elements, a dashpot with the prescribed constant will be attached at each grid point to which area A has been assigned.

IMPLEMENTING THE ANALOG FOR COMPUTING

With the basic ingredients of the structural analog described, there remains only to make a computation using it. The problem selected for solution is to find the scattered pressure generated on the surface of an infinite rigid cylinder of radius a = 0.5 meter by a plane wave propagating in the negative x-direction

(Figure 3) and having a maximum fluid particle velocity $\partial\phi_\infty/\partial x = V_x = -1$ in that direction. The infinite cylinder was chosen because analytically derived solutions are available for this case.[3]

Because of the shell's rigidity, only the exterior field need be modeled with finite elements. The presence of the shell is implicit in the shape of the interior fluid boundary and the inner boundary condition generated by this shape.

Consider now the details of setting up the finite-element model. As stated previously (page 3), the analogy specifies that the fluid surrounding the structure be modeled with two-dimensional plane stress elements having specially assigned material properties. The NASTRAN computer program was selected as the solver for the finite-element formulation, and the elements used to model the fluid are the CQDMEM elements. Since the structure-fluid interface is circular, it is convenient to use a polar configuration of elements to model the fluid (Figure 4). Symmetry permits

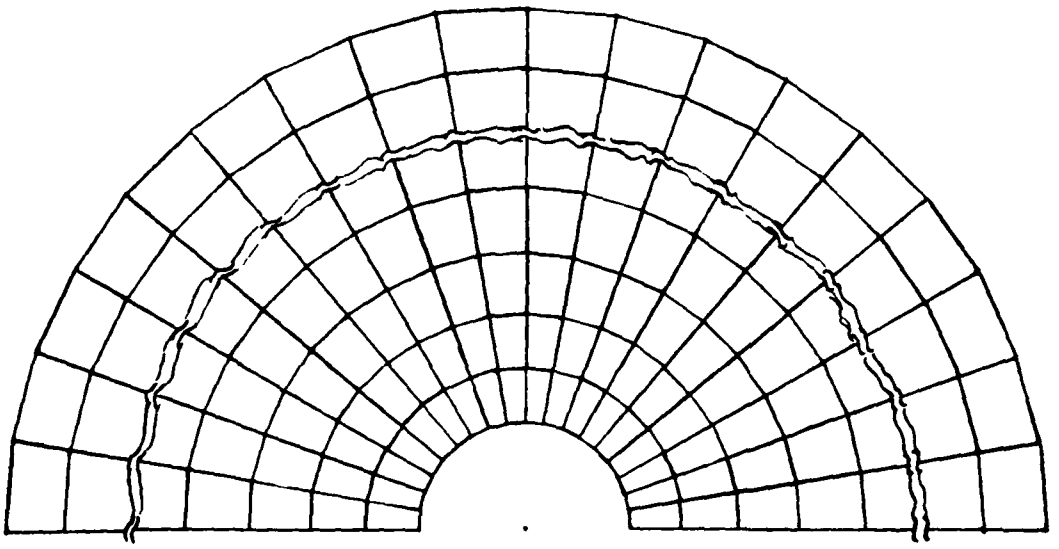

Figure 4 - Finite-Element Model of External Fluid

modeling only the upper half-plane. A perspective view of a typical field element is shown in Figure 5. The values for Young's modulus E_e, density ρ_e, and Poisson's ratio ν_e are computed from the expressions for material constants[2]

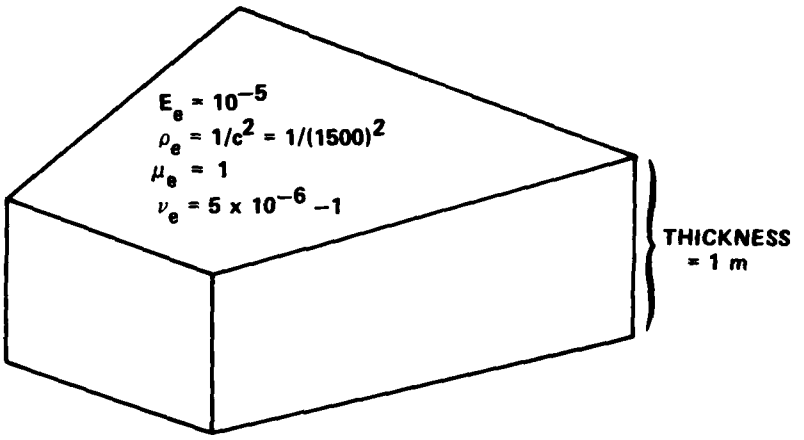

Figure 5 - Typical Membrane Element Used to Model Fluid

$$E_e = \beta\ \mu_e$$

$$\nu_e = 1/2\ \beta - 1 \qquad (16)$$

$$\rho_e = \mu_e \cdot \frac{1}{c^2}\ (c = \text{sound speed in fluid})$$

required to bring about the analogy for the two-dimensional case. In particular, the shear modulus μ_e is taken as unity, and β is chosen small compared to unity but not so small that $1+\beta$ is numerically indistinguishable from unity (e.g., $\beta=10^{-5}$).[2] An arbitrary thickness of unity is assigned to the membrane element. The subscript "e" signifies that these constants are artificial constants belonging to the elements which model the fluid.

Figure 6 depicts the inner fluid boundary in perspective to illustrate the discretization of the boundary surface and the application of the inner boundary condition. The angle α is determined by the spacing of elements around the circumference. Shaded areas of the two faces indicate the area $A = 1/2\ \text{Area}_1 + 1/2\ \text{Area}_2$ assigned to the central grid point. F_x at each grid point has the value indicated by Equation (6) with $\mu_e = 1$, A is the area assigned to the grid point as shown, and V_n the component of scattered velocity in the outward (into the fluid)

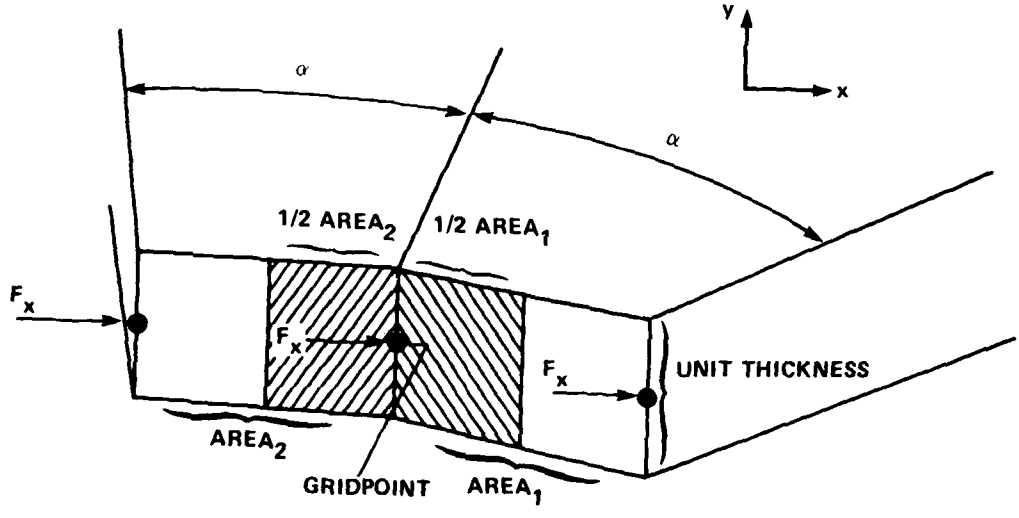

Figure 6 - Discretized Inner Fluid Boundary

direction normal to the structural surface. V_n (Figure 3) is easily determined by a simple cosine projection of the incident velocity vector v_x, which is assumed to be unity, onto the outward unit normal to the surface. For ease of specifying the inner boundary load, NASTRAN's facility for handling frequency dependent loads is used in the generalized form

$$\{p(f)\} = \{AB(f)e^{i[\phi(f)+\theta-2\pi f\tau]}\} \tag{17}$$

where f = frequency

θ = phase angle

τ = time delay

Figure 7 shows that the delay between the times at which a plane wave traveling in the negative x-direction intersects P_1 and P_2 equals the time to travel the distance d at speed c, so that $\tau = a(1-\cos\theta)/c$. If the incident wave is represented by

$$v(x,t) = V(x)e^{i\omega(t-\tau)} \quad (V(x) \text{ is magnitude}) \tag{18}$$

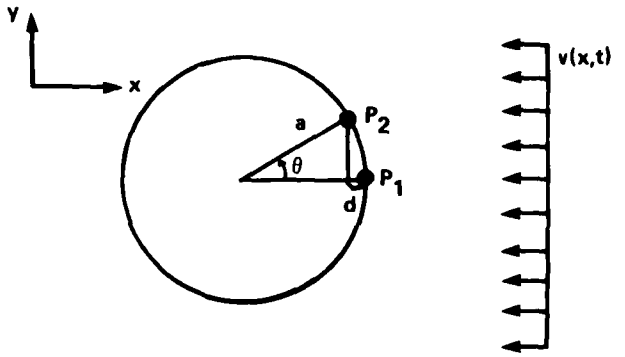

Figure 7 - Diagram for Computing Time Delay

then

$$v_n(x,t) = V(x) \cos\theta \, e^{-i\omega\tau} \, e^{i\omega t} \tag{19}$$

or, suppressing the time dependence,

$$v_n(x)_{\text{steady-state}} = V(x) \cos\theta \, e^{-i\omega\tau} \tag{20}$$

from which the applied force is

$$F_x = - A \, v_n(x) = - A \, V(x) \cos\theta \, e^{-i\omega\tau} \tag{21}$$

For $V(x) = 1$

$$F_x = - A \cos\theta \, e^{-i\omega\tau} \quad (A = \text{area}) \tag{22}$$

The last expression is nicely obtained from the generalized form (Equation (17)) by taking $B(f) \equiv 1$, with $\phi(f) = 0$ and $\theta = 0$, and the constant term equal to $-A \cos \theta$.

Figure 8 illustrates the discretization of the outer boundary (artificial) and application of the wave absorbing condition with dashpots. The dashpot constant at each grid point is the area assigned to the grid point, A = 1/2 Area_1 + 1/2 Area_2, divided by the sound speed c. NASTRAN's CDAMP2 cards are used to specify the constants.

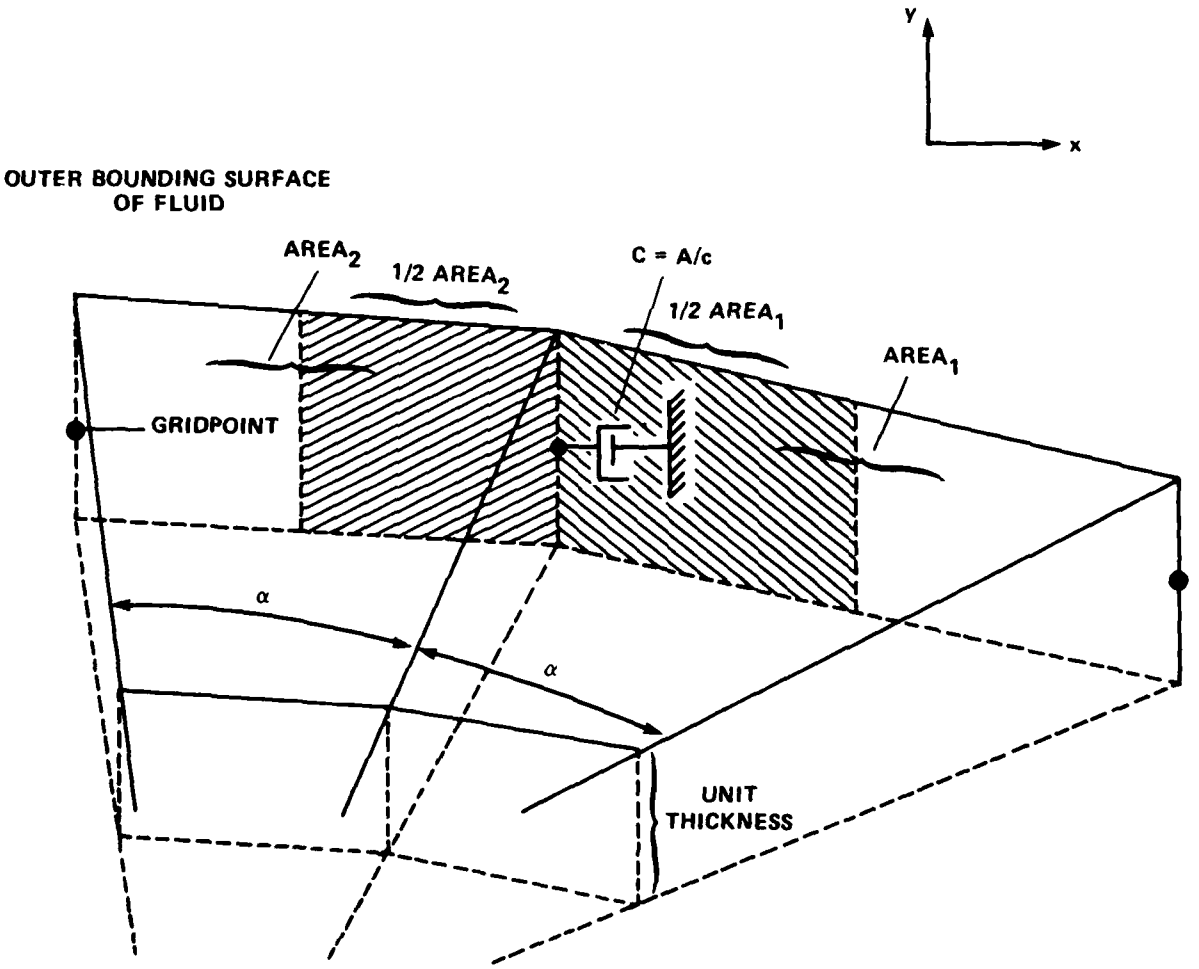

Figure 8 - Discretized Outer Fluid Boundary

As previously noted (page 6) the effectiveness of a plane-wave-absorbing boundary depends on its distance from the radiating (or scattering) surface. The present work uses the guideline for placing exterior boundaries reported by A.J. Kalinowski.[4] According to this guideline, a plane wave absorbing boundary placed 1.5 wavelengths from the structural surface will absorb 99.7 percent of outgoing waves, and a boundary placed one wavelength away will absorb 99.2 percent. This guideline for two-dimensional applications is based on consideration of the distance at which cylindrical waves spreading outward from an infinite line source may be assumed to be nearly plane waves.[4]

Another guideline[4] considered in establishing the fluid model relates to selection of element dimensions. With CQDMEM elements, the guideline recommends a minimum length in the radial direction (Figure 4) of at least one-sixth wavelength.

For the first calculations of both rigid and elastic scattering, it was convenient to use the automatic finite element modeling program GPRIME[6] to generate the CQDMEM meshes such as those shown in Figure 4. The particular submodule of GPRIME involved is GGEN, which provides two-dimensional capabilities. To this automatically generated portion of NASTRAN's BULK DATA were added constraint conditions, inner and outer boundary condition data, and the incident wave frequency. In accord with the analogy, all degrees of freedom except displacement in the x-direction were constrained at every grid point in the fluid. With these data, NASTRAN sets up and solves the matrix equation

$$[Q]\ \{\ddot{U}\} + [C]\ \{\dot{U}\} + [H]\ \{U\} = \{f\} \tag{23}$$

where [Q] is the inertia matrix for the fluid

[C] is the symmetric damping matrix for the fluid which arises from the radiation condition on the artificial outer boundary

[H] is the "stiffness" matrix for the fluid

From the correspondence between displacement and potential (Equation (3)) and the relation of acoustic pressure to potential (Equation (8)), the fluid pressure solution can be recovered from the "displacement" or "velocity" computed by NASTRAN. If displacement is selected, as was done here, pressure is obtained by

$$p = -i\omega\rho\ U \tag{24}$$

Normalizing by $\rho c V_o$, where V_o is an arbitrary reference velocity,

gives

$$\bar{p} = - ik U \tag{25}$$

CALCULATIONS OF RIGID SCATTERING

Modeling of the fluid region for the rigid-body calculations proceeded by first locating the boundary for the exterior fluid and then, based on the boundary location criterion (page 13) estimating the frequencies of scattering that might reasonably be handled with this boundary. The distance between shell surface and outer boundary was chosen to be ~10 m (actually 10.0889 m). The criterion suggests that a boundary at this distance will be a good absorber if the distance is 1 or 1.5 wavelengths of the scattered pressure. Since the wavelength $\lambda = 2\pi/k$, where $k = \omega/c$, the boundary distance was expected to be adequate for frequencies of 150 and 225 Hz, depending on whether it represented ~1 or 1.5 λ.

A finite element mesh was generated for the region between shell and outer field boundary consisting of 19 circumferential bands of 18 CQDMEM elements each. A picture of this mesh obtained through use of the STAGING program[7] is shown in Figure 9. A 150-Hz scattering calculation was run with this mesh and the calculated surface pressures are seen in Figure 10 to be in excellent agreement with results from an analytic formula[3] which was implemented for automatic calculation in a special purpose program SCAT1.

To obtain results at 225 Hz comparable to those at 150 Hz, it was necessary to increase the density of the finite element mesh. This was accomplished by subdividing circumferential bands of elements beginning at the fourteenth band out from the shell surface and extending to the outer boundary (Figure 11). Calculated pressures are shown in Figure 12.

SCATTERING FROM AN EMPTY ELASTIC CYLINDER

STRUCTURAL ANALOG FOR FLUID-STRUCTURE INTERACTION (SYMMETRIC POTENTIAL FORMULATION)

The analogy used for scattering calculations when the cylindrical shell is allowed to deform is based on a finite element formulation[5] for coupled fluid-structure interaction in which pressure is the single unknown at grid points in the fluid,

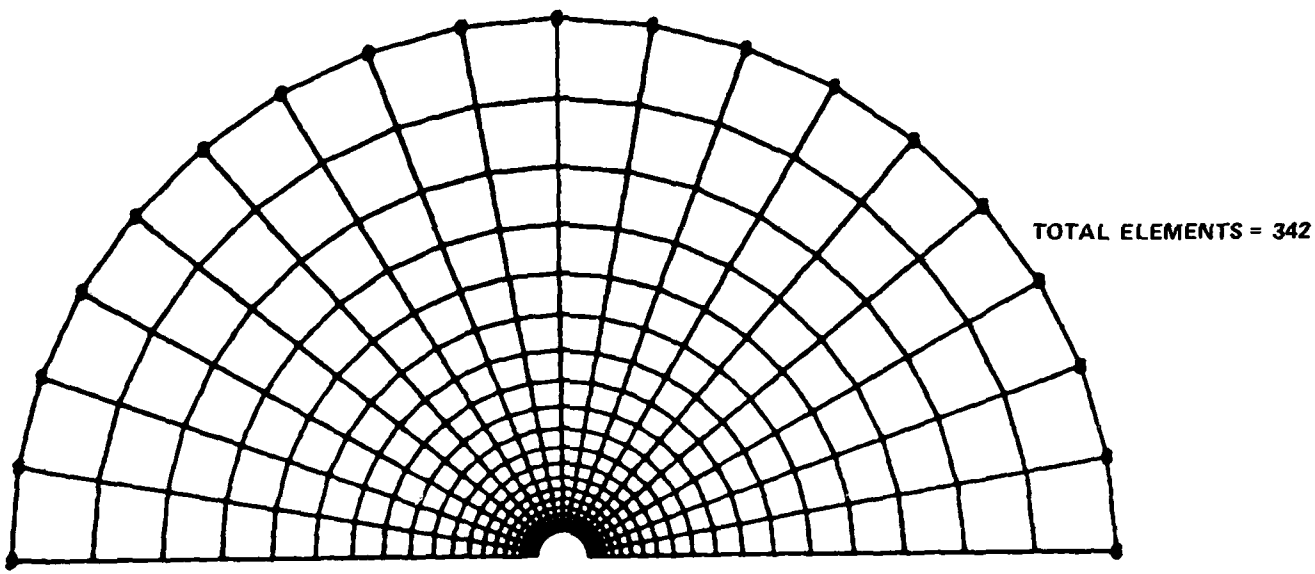

Figure 9 - Finite-Element Mesh for 150 Hertz Rigid Scattering Calculation

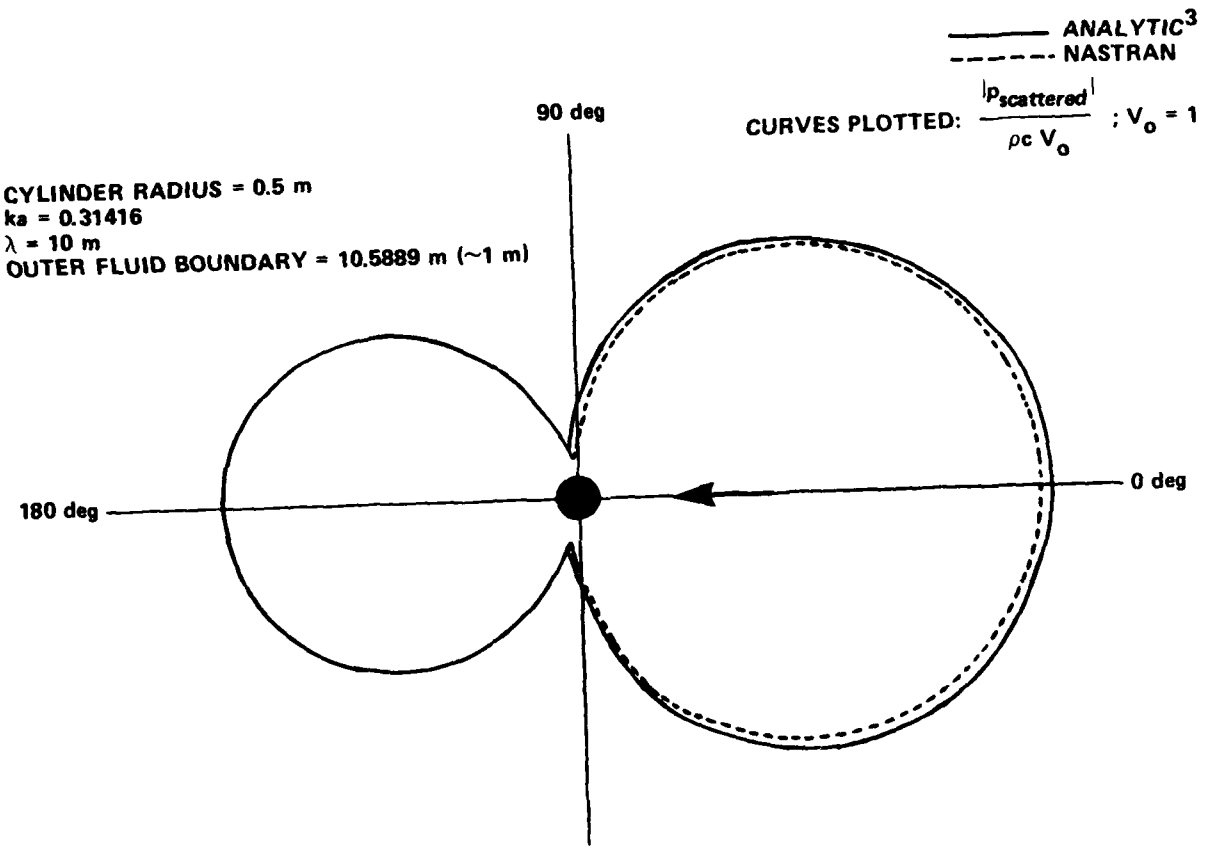

Figure 10 - Calculated Pressures on the Surface of a Cylinder for 150 Hertz Rigid Scattering

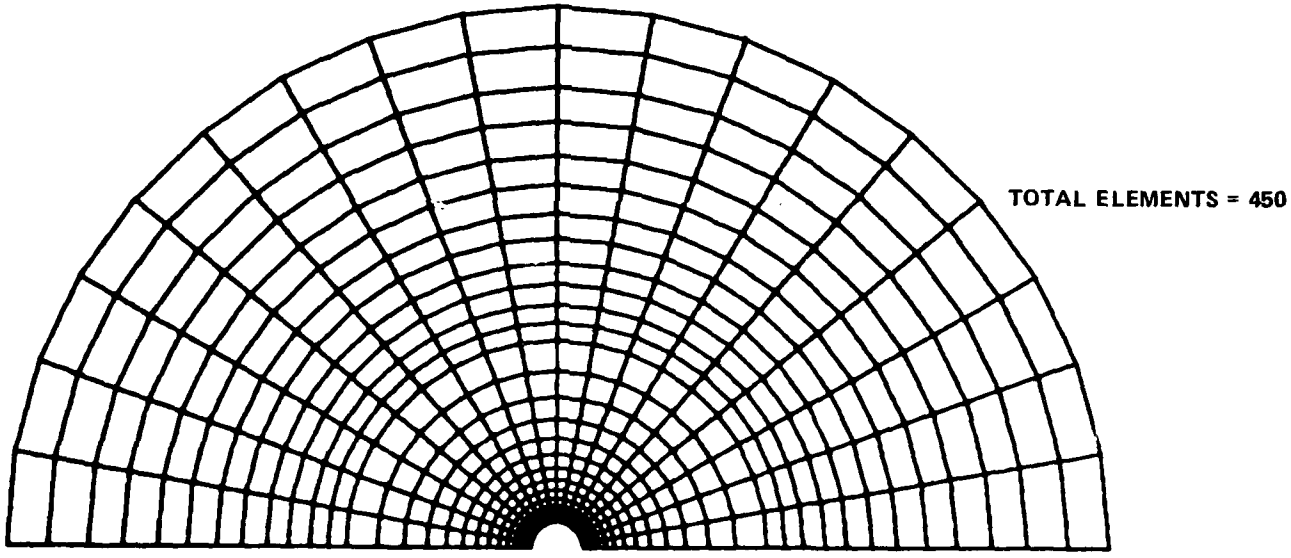

Figure 11 - Finite-Element Mesh for 225 Hertz Rigid Scattering Calculation

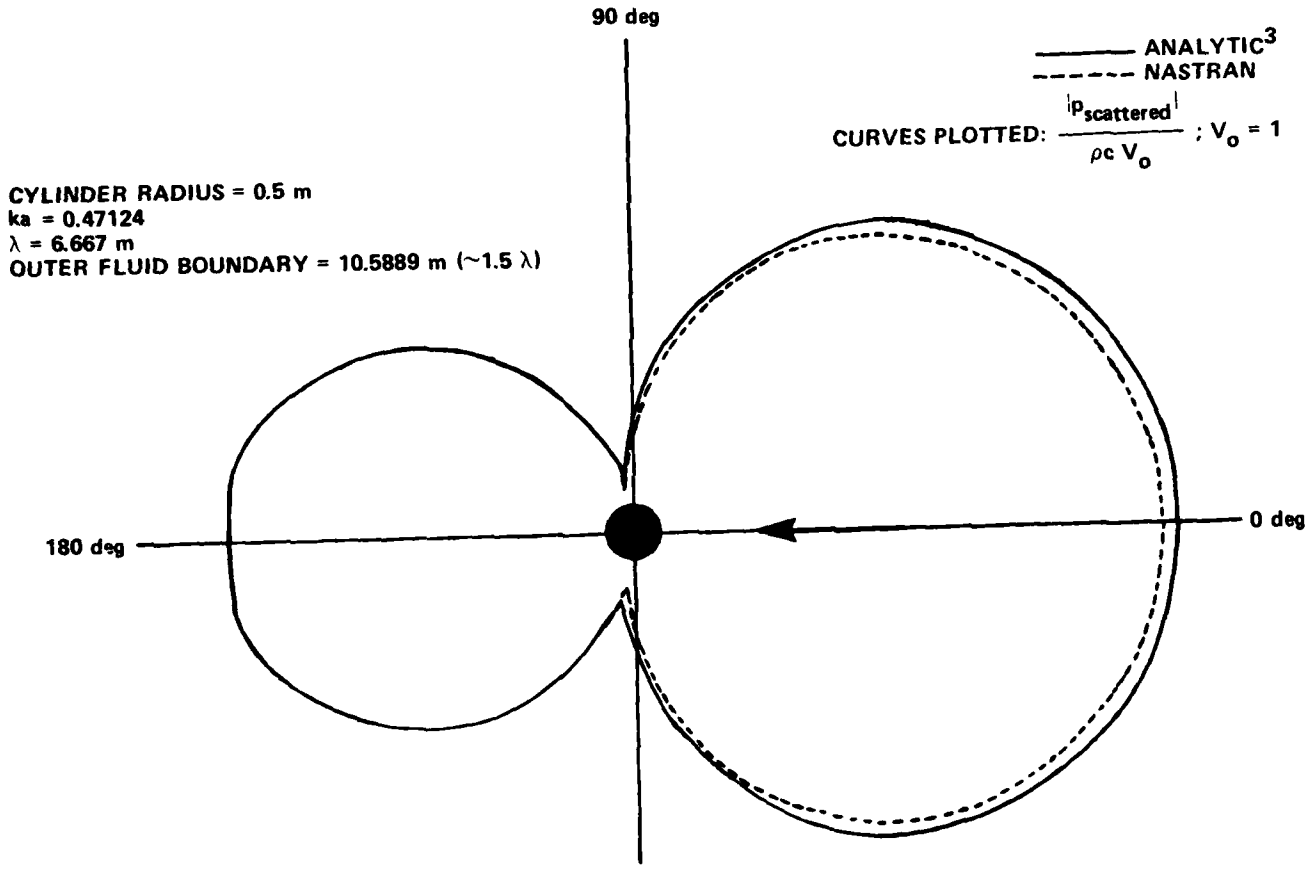

Figure 12 - Calculated Pressures on the Surface of a Cylinder for 225 Hertz Rigid Scattering

$$\begin{bmatrix} \underset{\sim}{M} & \underset{\sim}{0} \\ -\rho\underset{\sim}{A}^T & Q \end{bmatrix} \begin{Bmatrix} \ddot{\underset{\sim}{U}} \\ \ddot{\underset{\sim}{p}} \end{Bmatrix} + \begin{bmatrix} \underset{\sim}{B} & \underset{\sim}{0} \\ \underset{\sim}{0} & \underset{\sim}{C} \end{bmatrix} \begin{Bmatrix} \dot{\underset{\sim}{U}} \\ \dot{\underset{\sim}{p}} \end{Bmatrix} + \begin{bmatrix} \underset{\sim}{K} & \underset{\sim}{A} \\ \underset{\sim}{0} & \underset{\sim}{H} \end{bmatrix} \begin{Bmatrix} \underset{\sim}{U} \\ \underset{\sim}{p} \end{Bmatrix} = \begin{Bmatrix} \underset{\sim}{f}_1 \\ \underset{\sim}{f}_2 \end{Bmatrix} \tag{26}$$

where $\underset{\sim}{U}$ is the vector of displacement components in the structure

$\underset{\sim}{p}$ is the vector of pressures at fluid grid points

$\underset{\sim}{M}$ is the structural mass matrix

$\underset{\sim}{K}$ is the structural stiffness matrix

$\underset{\sim}{B}$ is the symmetric damping matrix for the structure

ρ is the fluid mass density

A is the area matrix which converts fluid pressures at fluid-structure interface grid points to structural loads, and

$\underset{\sim}{H}$, $\underset{\sim}{C}$, and $\underset{\sim}{Q}$ are as previously defined (page 13)

The right-hand side represents the vectors $\underset{\sim}{f}_1$ and $\underset{\sim}{f}_2$ of known forces acting on the structure and fluid, respectively. It is seen that, without the coupling term $-\rho\underset{\sim}{A}^T$, the matrix equation for p has exactly the form given on page 13 for the velocity potential, reflecting the fact that both pressure and velocity potential satisfy the wave equation for the field.

Although Equation (26) is amenable to solution by a general structural analysis computer program such as NASTRAN, the present investigation uses a reformulation[8] of the problem which yields a symmetric matrix system. The symmetrization process proceeds as follows: dividing the second partition of Equation (26) by $-1/\rho$ and integrating the resulting equations in time yields

$$\begin{bmatrix} \underset{\sim}{M} & \underset{\sim}{0} \\ \underset{\sim}{0} & \underset{\sim}{0} \end{bmatrix} \begin{Bmatrix} \ddot{\underset{\sim}{U}} \\ \underset{\sim}{0} \end{Bmatrix} + \begin{bmatrix} \underset{\sim}{B} & \underset{\sim}{0} \\ \underset{\sim}{A}^T & -\underset{\sim}{Q}/\rho \end{bmatrix} \begin{Bmatrix} \dot{\underset{\sim}{U}} \\ \dot{\underset{\sim}{p}} \end{Bmatrix} + \begin{bmatrix} \underset{\sim}{K} & \underset{\sim}{A} \\ \underset{\sim}{0} & -\underset{\sim}{C}/\rho \end{bmatrix} \begin{Bmatrix} \underset{\sim}{U} \\ \underset{\sim}{p} \end{Bmatrix} + \begin{bmatrix} \underset{\sim}{0} & \underset{\sim}{0} \\ \underset{\sim}{0} & -\underset{\sim}{H}/\rho \end{bmatrix} \begin{Bmatrix} \underset{\sim}{0} \\ \int_0^t \underset{\sim}{p}\, dt \end{Bmatrix}$$

$$= \begin{Bmatrix} \underset{\sim}{f}_1 \\ -\frac{1}{\rho} \int_0^t \underset{\sim}{f}_2\, dt \end{Bmatrix} \tag{27}$$

Introducing a new unknown vector

$$\underset{\sim}{q} = \int_0^t \underset{\sim}{p}\, dt \tag{28}$$

from which

$$\dot{\underset{\sim}{q}} = \underset{\sim}{p} \tag{29}$$

and

$$\ddot{\underset{\sim}{q}} = \dot{\underset{\sim}{p}} \tag{30}$$

and substituting into Equation (27) gives the following system of equations which, in the literature,[8] is referred to as the "symmetric potential formulation,"

$$\begin{bmatrix} \underset{\sim}{M} & \underset{\sim}{0} \\ \underset{\sim}{0} & -\underset{\sim}{Q}/\rho \end{bmatrix} \begin{Bmatrix} \ddot{\underset{\sim}{U}} \\ \ddot{\underset{\sim}{q}} \end{Bmatrix} + \begin{bmatrix} \underset{\sim}{B} & \underset{\sim}{A} \\ \underset{\sim}{A}^T & -\underset{\sim}{C}/\rho \end{bmatrix} \begin{Bmatrix} \dot{\underset{\sim}{U}} \\ \dot{\underset{\sim}{q}} \end{Bmatrix} + \begin{bmatrix} \underset{\sim}{K} & \underset{\sim}{0} \\ \underset{\sim}{0} & -\underset{\sim}{H}/\rho \end{bmatrix} \begin{Bmatrix} \underset{\sim}{U} \\ \underset{\sim}{q} \end{Bmatrix} = \begin{Bmatrix} \underset{\sim}{f}_1 \\ \underset{\sim}{g}_2 \end{Bmatrix} \tag{31}$$

where

$$g_2 = -\frac{1}{\rho} \int_0^t \underset{\sim}{f}_2\, dt$$

The terminology "symmetric potential formulation" arises from the fact that q (Equation (29)) differs from the velocity potential ϕ (Equation (8)) by only the constant multiplier ρ.

Consideration is next given to the form that Equation (31) takes for elastic scattering. To derive this form it is convenient to begin with the expression[3] for the total pressure scattered from an elastic body ensonified by an incident plane wave of pressure p_i,

$$p_t = p_i + p_{se} \tag{32}$$

where p_{se} is pressure scattered by an elastic boundary. p_{se} is then represented[3] as the sum

$$p_{se} = p_{s\infty} + p_r \tag{33}$$

where $p_{s\infty}$ is pressure scattered by the rigid surface and p_r is the pressure radiated from elastic motion of the shell. Then by substitution of Equation (33) into Equation (32),

$$p_t = p_i + p_{s\infty} + p_r \tag{34}$$

Since Equation (34) is the pressure at the interface between structure and fluid, the resultant forces against the shell surface at grid points of a finite element model are

$$\underset{\sim}{F}_l = - \underset{\sim}{A}\, \underset{\sim}{p}_i - (\underset{\sim}{p}_{s\infty}+\underset{\sim}{p}_r)\, \underset{\sim}{A} = - \underset{\sim}{A}\, \underset{\sim}{p}_i - \underset{\sim}{A}\, \underset{\sim}{p}_{se} \tag{35}$$

where A is the matrix of areas associated with grid points.
The force acting on the inner fluid boundary is obtained from the boundary condition

$$\frac{\partial p}{\partial n} = - \rho\, \ddot{U}_n \tag{36}$$

where U_n is the normal component of shell displacement.
Substituting Equation (34) for total pressure gives

$$\frac{\partial p_t}{\partial n} = \frac{\partial p_i}{\partial n} + \frac{\partial p_{s\infty}}{\partial n} + \frac{\partial p_r}{\partial n} = - \rho\, \ddot{U}_n \tag{37}$$

from which

$$\frac{\partial p_{s\infty}}{\partial n} + \frac{\partial p_r}{\partial n} = - \rho \ddot{U}_n - \frac{\partial p_i}{\partial n} \tag{38}$$

or

$$\frac{\partial p_{se}}{\partial n} = - \rho \ddot{U}_n - \frac{\partial p_i}{\partial n} \tag{39}$$

Substituting

$$\frac{\partial p_i}{\partial n} = - \rho \dot{v}_{i_n} \tag{40}$$

where v_{i_n} denotes the normal component of the incident wave's particle velocity, into Equation (39) gives

$$\frac{\partial p_{se}}{\partial n} = - \rho(\ddot{U}_n - \dot{v}_{i_n}) \tag{41}$$

In the analogy (pages 5-6), enforcement of a normal derivative condition on the scalar field variable at the structural surface is accomplished by application of a particular "load" against the inner surface boundary of the fluid. The condition described by Equation (41) is then obtained by imposing the load

$$\underset{\sim}{F}_2 = \mu_e \underset{\sim}{A}\rho(\ddot{\underset{\sim}{U}}_n - \dot{\underset{\sim}{v}}_{i_n}) = \underset{\sim}{A} \rho(\ddot{\underset{\sim}{U}}_n - \dot{\underset{\sim}{v}}_{i_n}) \tag{42}$$

at grid points of the finite element model, with $\underset{\sim}{A}$ a matrix of areas (of the fluid inner boundary surface) associated with the grid points, and v_{i_n} the normal component of particle velocity in the incident wave. Performing the integration of $\underset{\sim}{F}_2$ required by the symmetry formulation yields

$$\underset{\sim}{G}_2 = - \frac{1}{\rho} \int_o^t \underset{\sim}{F}_2 \, dt \approx - \underset{\sim}{A} \dot{\underset{\sim}{U}}_n + A \, v_{i_n} \tag{43}$$

and substituting $\underset{\sim}{p}_{se} = \dot{\underset{\sim}{q}}_{se}$ in Equation (35) yields

$$\underset{\sim}{F}_1 = - \underset{\sim}{A}\, \underset{\sim}{p}_i - \underset{\sim}{A}\, \dot{\underset{\sim}{q}}_{se} \tag{44}$$

The unknown components $- \underset{\sim}{A}\, \dot{\underset{\sim}{U}}_n$ and $- \underset{\sim}{A}\, \dot{\underset{\sim}{q}}_{se}$ in the fluid and shell loadings are moved to the left side of Equation (31) giving, respectively, the upper right and lower left partitions of the second, or damping, matrix. With the replacement of p_i by $-\rho c v_{i_x}$ (from the relationship between pressure and velocity in a plane wave propagating in the negative x-direction) the known components of $\underset{\sim}{G}_2$ and $\underset{\sim}{F}_1$ become the right-hand side of Equation (31)

$$\underset{\sim}{f}_1 = - \underset{\sim}{A}\, \underset{\sim}{p}_i = \rho c\, A\, v_{i_x} \tag{45}$$

$$\underset{\sim}{g}_2 = A\, v_{i_n} = A\, v_{i_x} \cos \theta \tag{46}$$

thus completing the symmetric formulation for plane wave scattering.

IMPLEMENTING THE SYMMETRIC POTENTIAL FORMULATION

Performing elastic scattering calculations with the formulation just described requires the following steps:

a. Construction of finite element models of the cylinder and its applied loads, and of the fluid with its applied loads and outer boundary conditions, and

b. Connection of the two models at their interface.

The details of these steps are outlined in this section.

A. Finite Element Models of Cylinder and Fluid

As a basis for discretizing the cylinder, a set of grid points is established around the upper half-plane circumference and these points are connected in pairs by bar elements (NASTRAN CBAR cards), Figure 13. Since only an arbitrary "slice" of the infinite cylinder is being modeled, the bar elements are assigned an arbitrary depth of 1 m. Since the cylinder is a real structure as opposed to the analog structure which represents the fluid, the cylinder's elements have the actual properties of its material. For this work, it was assumed that the cylinder is

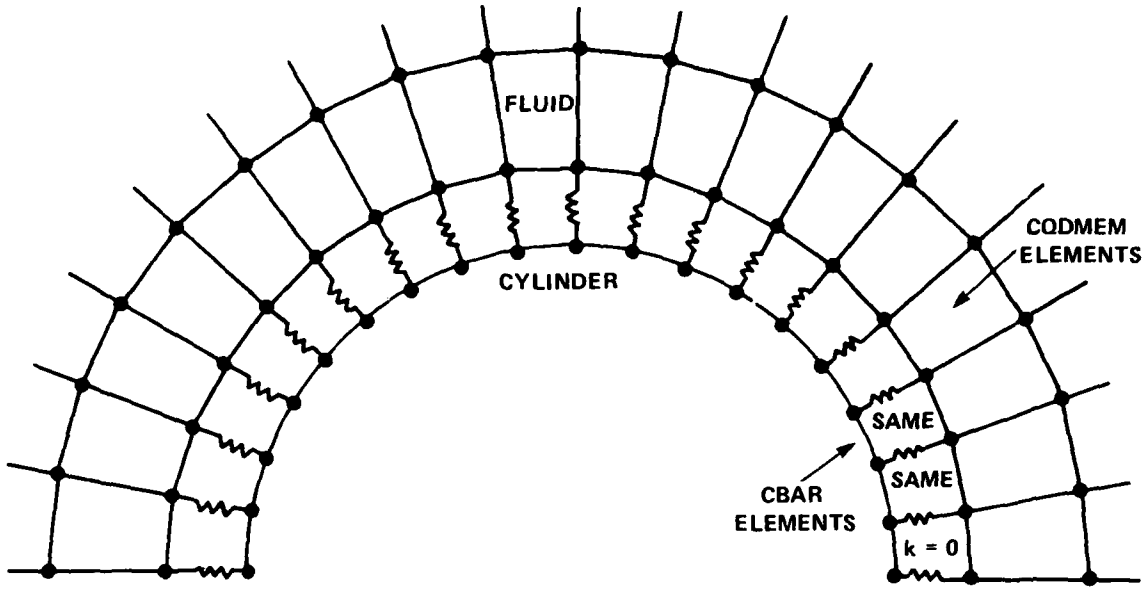

Figure 13 - Finite-Element Model of Structure-Fluid Interface for Submerged Empty Cylinder

steel, that it is 0.01 m thick (which makes it a "thin" shell), and that it has the following material properties:[9]

$$\text{density } \rho_s = 7700 \text{ kg/m}^3$$

$$\text{Young's modulus } E_s = 19.5 \times 10^{10} \text{ newtons/m}^2 \tag{47}$$

$$\text{Poisson's ratio } \nu_s = 0.28$$

For use in the calculations these properties must in turn be converted to their corresponding effective values for plane strain,

$$E_{s_{\text{plane strain}}} = \frac{E_{s_{\text{plane stress}}}}{1-\nu^2_{s_{\text{plane stress}}}} = 2.116 \times 10^{11}$$

$$\nu_{s_{\text{plane strain}}} = \frac{\nu_{\text{plane stress}}}{1-\nu_{\text{plane stress}}} = .38889 \tag{48}$$

These values of E_s and ν_s, along with thickness and ρ_s, are the data supplied on the property card for the CBAR elements.

The fluid finite element model is, as for rigid scattering, an assemblage of membrane elements such as the one shown in Figure 5. However, the material property constants for the elements must be altered to account for the division by $-\rho$ required for the symmetric formulation (Equation (31)). Thus, the following constants, given in Figure 5 are transformed to

$$E_e = -\frac{10^{-5}}{\rho}$$

$$\rho_e = -\frac{1}{\rho c^2} \qquad (49)$$

$$\mu_e = -\frac{1}{\rho}$$

where ρ is the actual density of seawater and has the value[9] 1026 kg/m^3. The dashpot constants (partition C in Equation (31)) on the outer boundary are also affected by the transformation, and their previous values of A/c (page 12) are replaced by $-A/\rho c$.

Equation (45) gives the load acting against the cylinder surface as simply $-\rho cA$, when $v_{i_x} = -1$. Comparing Equation (46) with Equation (6) shows that the load acting against the fluid surface is the same as that prescribed for rigid scattering.

B. Interface Connection of Cylinder and Fluid Models

Although the cylinder grid points and fluid inner boundary grid points are shown in Figure 13 to be spatially separated, they are actually coincident grid points in the model. The two sets do not have the same numbers. It is convenient for subsequent grid point resequencing by BANDIT[10] to tie such coincident points together with zero-stiffness springs so that BANDIT, which does not read the DMIG cards used, will see the structure and fluid models as connected. The actual coupling of the two models is accomplished by setting up the $\underset{\sim}{A}$ and $\underset{\sim}{A}^T$ partitions of the second matrix in Equation (31). The assignment of area to grid points has

already been shown in Figure 6 for the inner fluid boundary. The same manner of assignment is used for the cylindrical surface model which exactly matches that for the fluid, with the result that each of a pair of coincident grid points is assigned the same size area. Equations (43) and (44) show that the area associated with the structural grid point of a coincident pair multiplies only the normal component of the point's motion, whereas the area associated with the fluid point of the pair multiplies the single scalar degree of freedom associated with the fluid point.

NASTRAN's DMIG cards are used to specify, in terms of grid point numbers and component numbers, the locations (i,j) for inserting corresponding areas directly into the damping matrix.

To run the symmetric formulation, a special option, SYSTEM (77) = - 1, must be specified on the NASTRAN card. This option, which is available only with the Center's version of NASTRAN, allows the use of negative values for E_e and μ_e (Equation (49)).

CALCULATIONS OF ELASTIC SCATTERING

The fluid mesh (Figure 11) for the 225-Hz rigid scattering run was used as a basis for the first elastic scattering calculation at the same frequency. The material properties of the membrane elements and dashpot constants on the outer boundary were divided by - ρ, and the inner boundary grid points were used to define the modeling of the cylinder; i.e., the surface between 0 and 180 deg was subdivided into grid points 10 deg apart which were then connected by 18 bar elements.

Velocity output was requested from the NASTRAN run, since it is this quantity at fluid grid points that is analogous to pressure, as indicated in Equation (29). Computed pressures at the cylinder surface are compared (Figure 14) with results obtained from an analytic formulation[3] coded by the author in a special purpose program SCAT2. In the range 0 to 90 deg the numerical result differs from the analytic by essentially a constant, about 6 percent. The results obtained with this fluid mesh for rigid scattering (Figure 12) strongly indicate that for some reason the mesh may not perform equally well for rigid and elastic scattering. This possibility was confirmed by increasing the radial density of elements in the fluid mesh (Figure 15) and recalculating. The results (Figure 16) deviate from the analytic curve by about 3 percent.

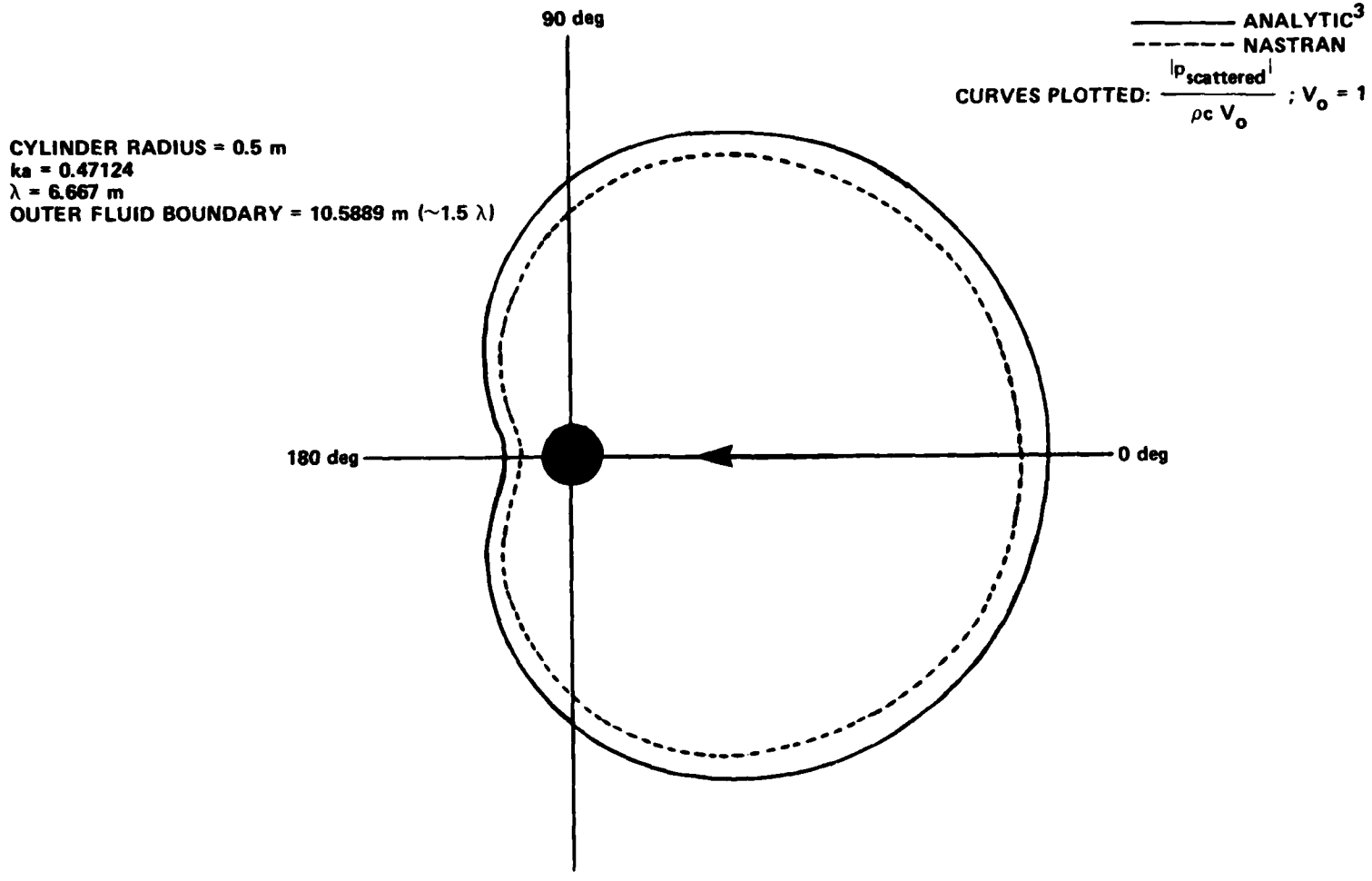

Figure 14 - Calculated Pressures on the Surface of an Elastic Cylinder for Incident Wave Frequency 225 Hertz Using Fluid Mesh in Figure 11

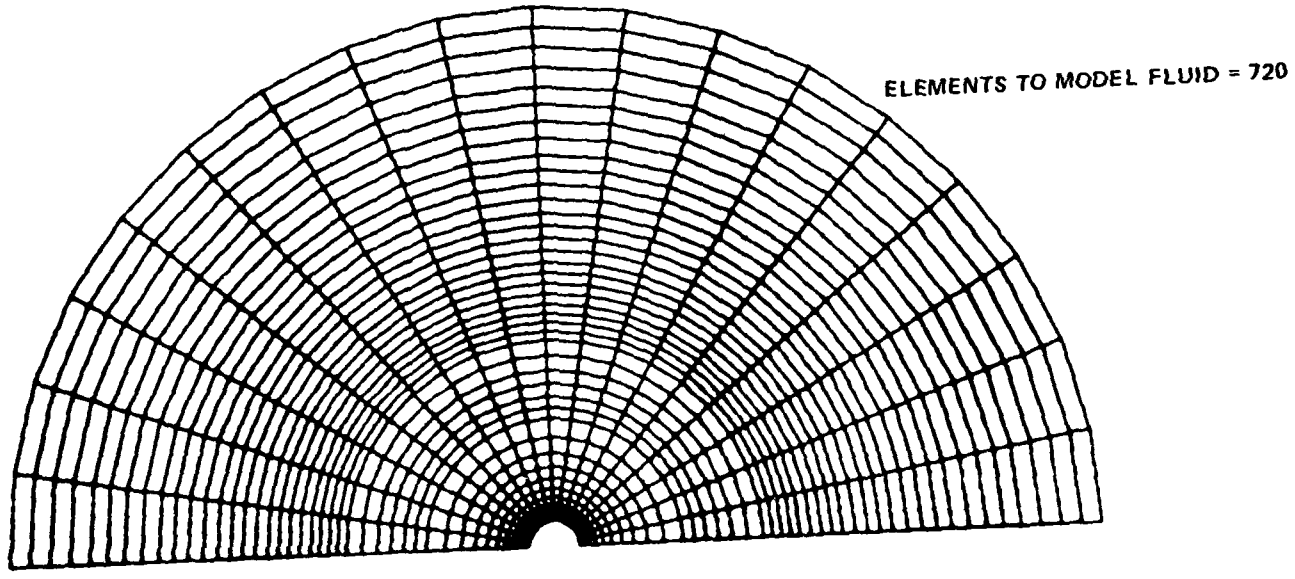

Figure 15 - Refinement of Finite-Element Mesh in Figure 11 for 225 Hertz Elastic Scattering Calculation

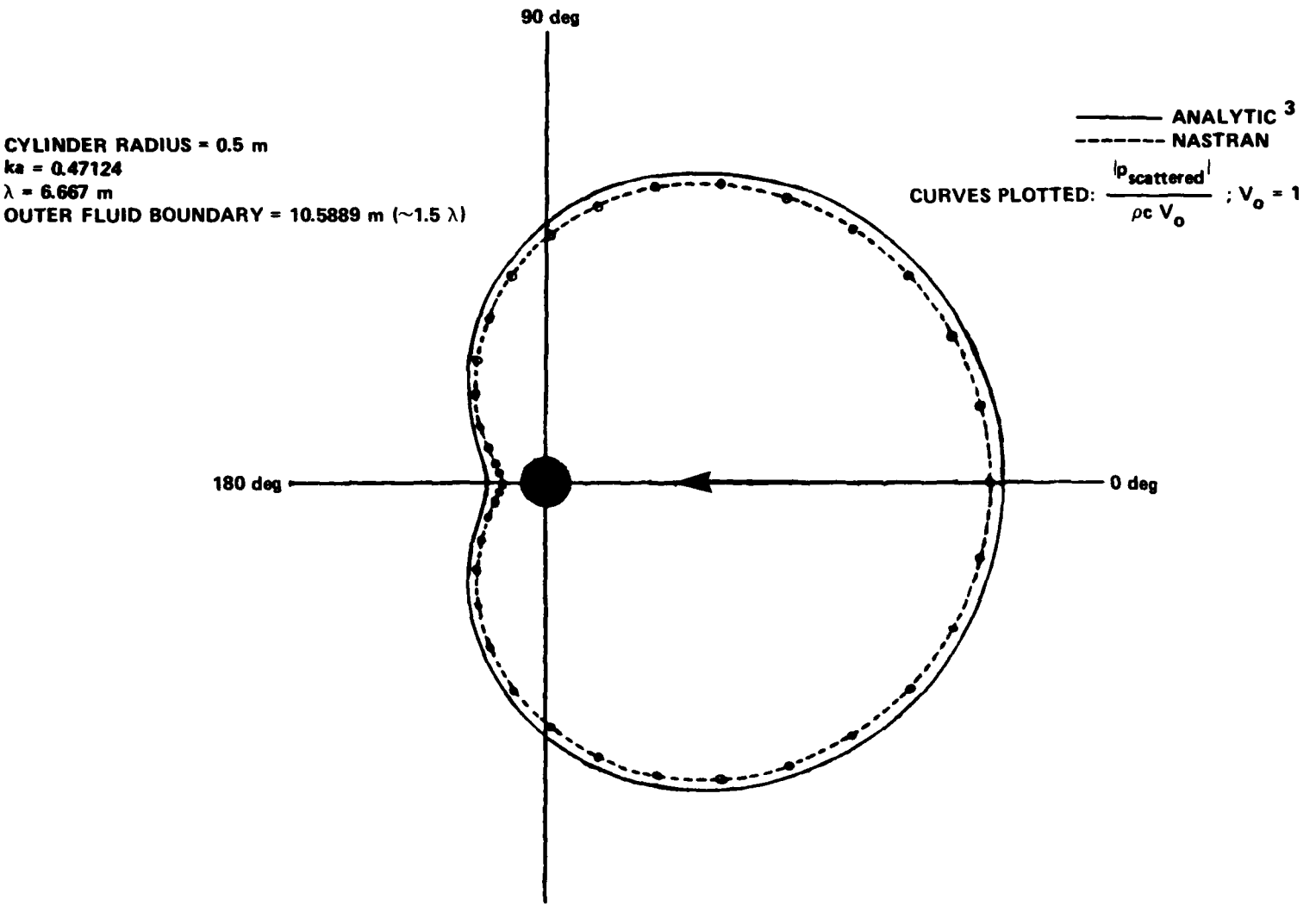

Figure 16 - Calculated Pressures on the Surface of an Elastic Cylinder for Incident Wave Frequency 225 Hertz Using Refined Fluid Mesh in Figure 15

Although reasonably good results were obtained thus far, the results were for frequencies far below the intended range of interest, 1 to 20 kc. It was, therefore, essential for the ultimate usefulness of the method to gain some insight into its performance at the higher frequencies.

Before the results obtained at higher frequencies are summarized, a description is offered of the modeling strategy and some software developed to assist in generating the fluid-structure models for these frequencies.

When the structure is modeled, it is very helpful to have some idea of its natural frequencies and modes, since the modeling of the structural surface should be sufficient to resolve modes that dominate its response. Although this information is not generally known for submerged bodies of arbitrary shape, it is known approximately for infinite hollow thin cylinders. The particular formulation used here is from Feit and Junger[3] [Equation (10.31), page 272] and provides, for any mode number $n > 0$, an estimate of the submerged natural frequency. The mode designator n counts the number of full sine waves (radial or transverse motion) around the circumference of the cylinder. If it is assumed that eight grid points per full sine wave are adequate to reproduce the wave, an initial estimate of $n/2 \times 8$ (n even) or $(n/2 + 1) \times 8$ (n odd) equally spaced grid points is obtained for the cylinder model at the corresponding natural frequency.

As previously noted (page 13) for the earlier calculations at low frequencies, the facilities of GPRIME[6] were used to generate automatically the fluid mesh to which were added manually the structural model, interface loadings, and fluid outer boundary condition. The updating was necessary because loading, damping, and "DMIG" data are not generated by GPRIME. At low frequencies the updating was no real problem, since relatively few (< 20) elements were needed to represent the boundary surfaces. In the higher frequency ranges, however, elements at the interface boundaries can easily number in the hundreds, making manual updating tedious. Therefore, a special purpose generator GEN was developed which produces, except for a few cards, the entire bulk data deck required for the NASTRAN run. The generator also provides for modeling transition zones in the fluid mesh, which facilitates reduction of elements in the circumferential direction between the structural and fluid models.

Figures 17-25 summarize the final results from three sets of calculations in the frequency range of interest. The results shown in each case except the last are

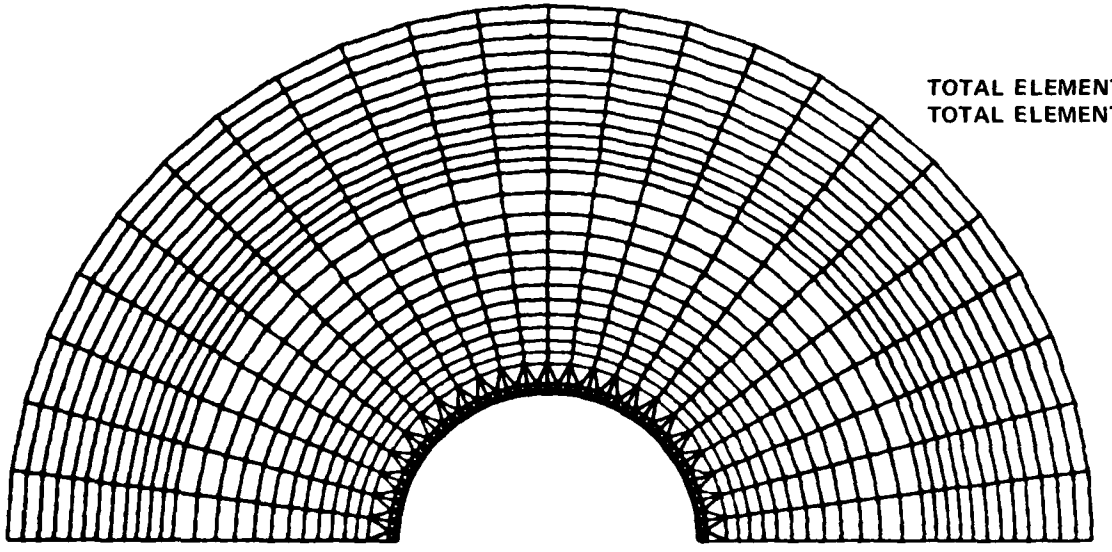

Figure 17 - Finite-Element Mesh for 2100 Hertz Elastic Scattering Calculation

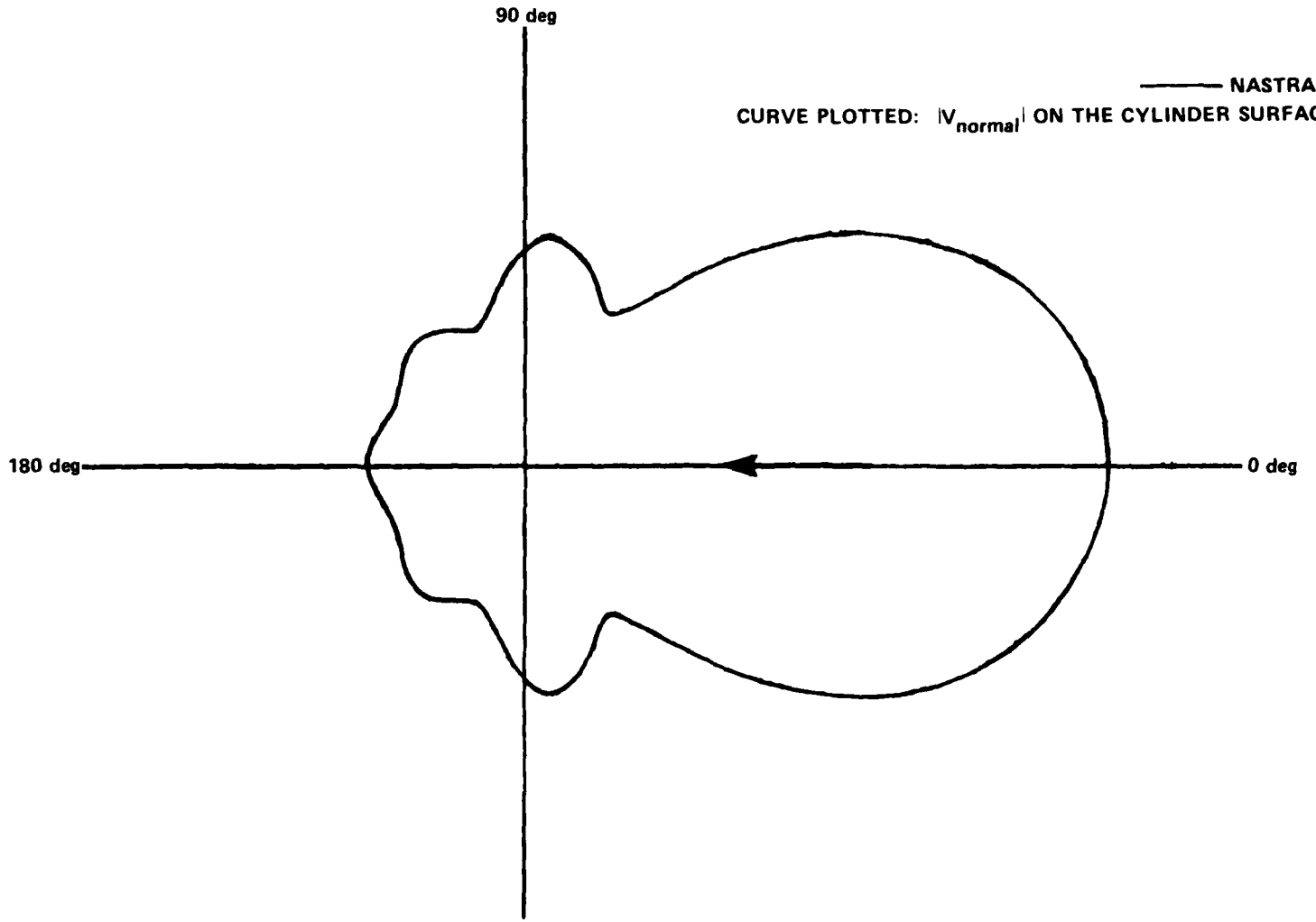

Figure 18 - Calculated Velocities on the Surface of a Cylinder for 2100 Hertz Elastic Scattering

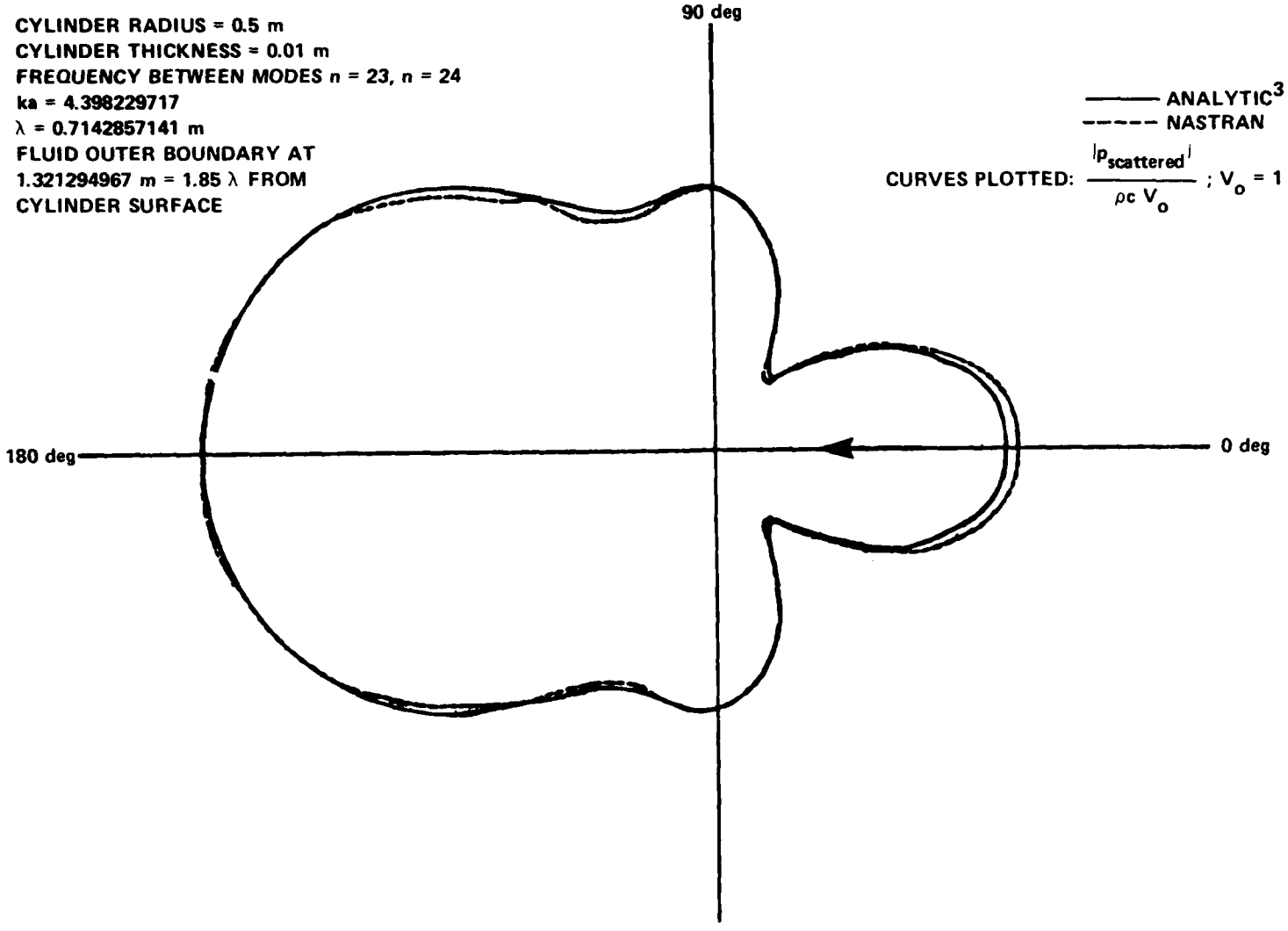

Figure 19 - Calculated Pressures on the Surface of a Cylinder for 2100 Hertz Elastic Scattering

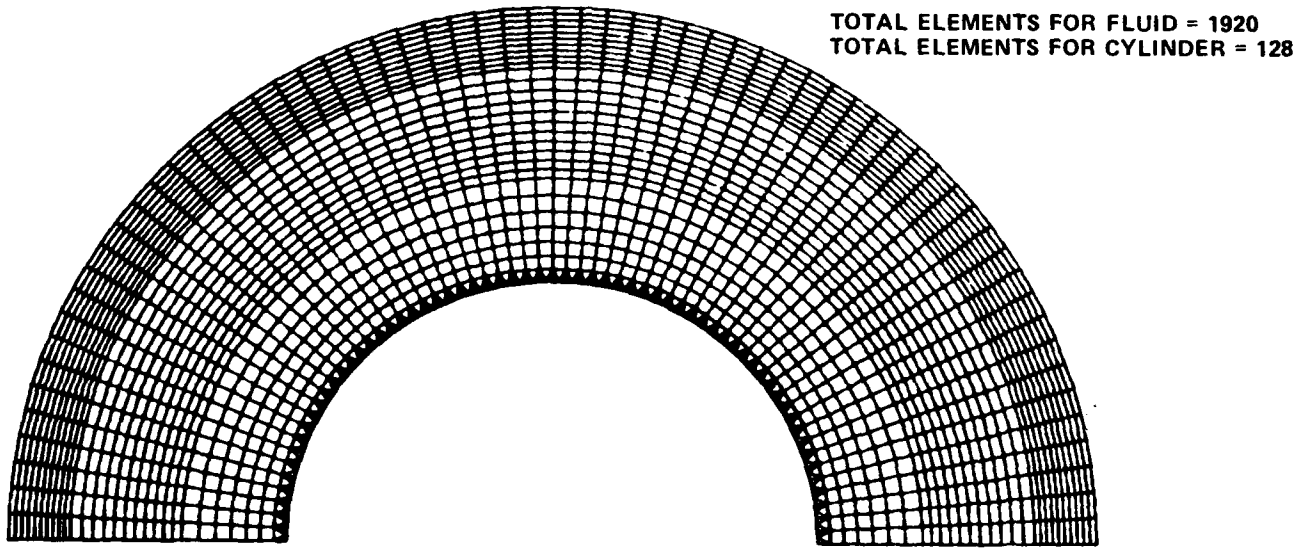

Figure 20 - Finite-Element Mesh for 4100 Hertz Elastic Scattering Calculation

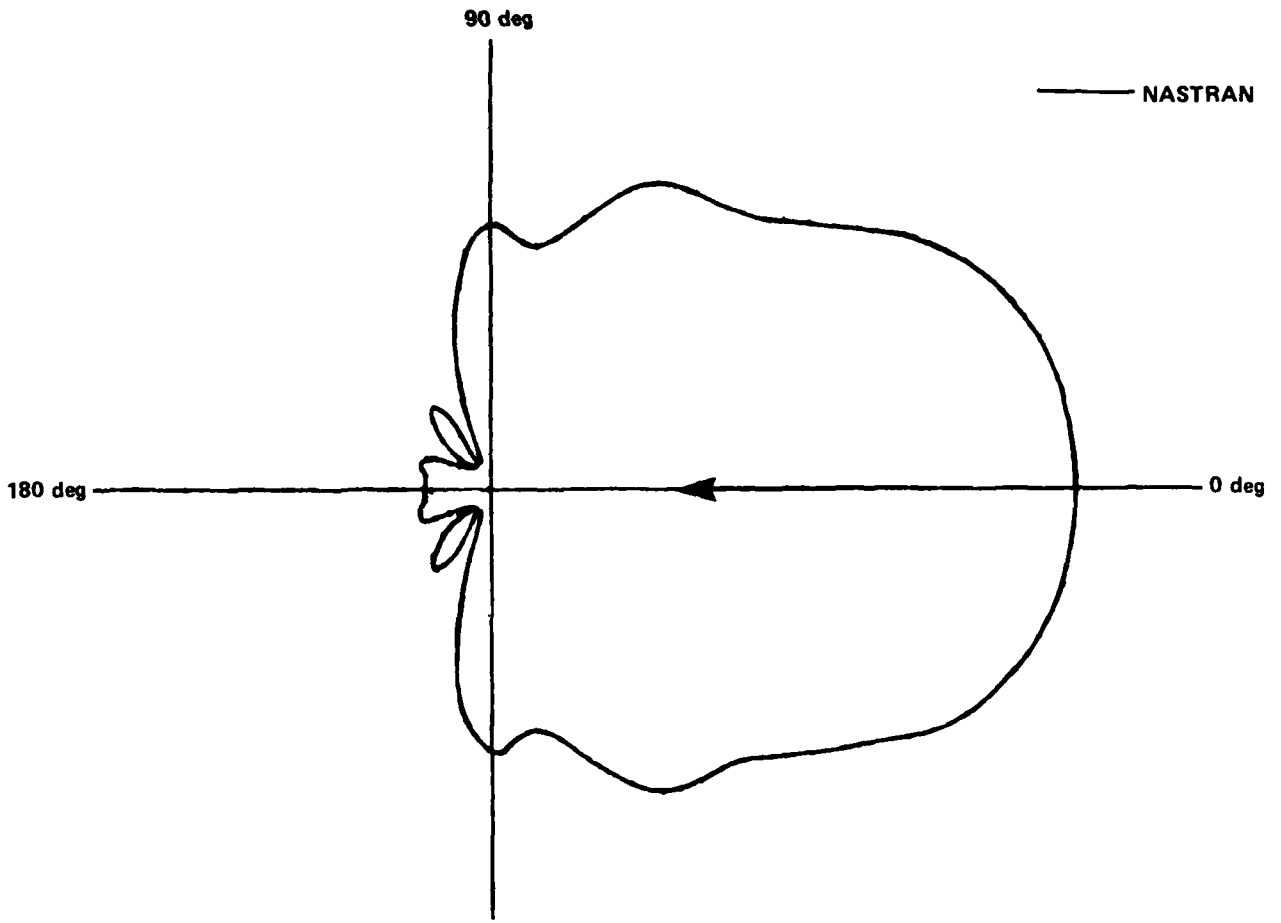

Figure 21 - Calculated Velocities on the Surface of a Cylinder for 4100 Hertz Elastic Scattering

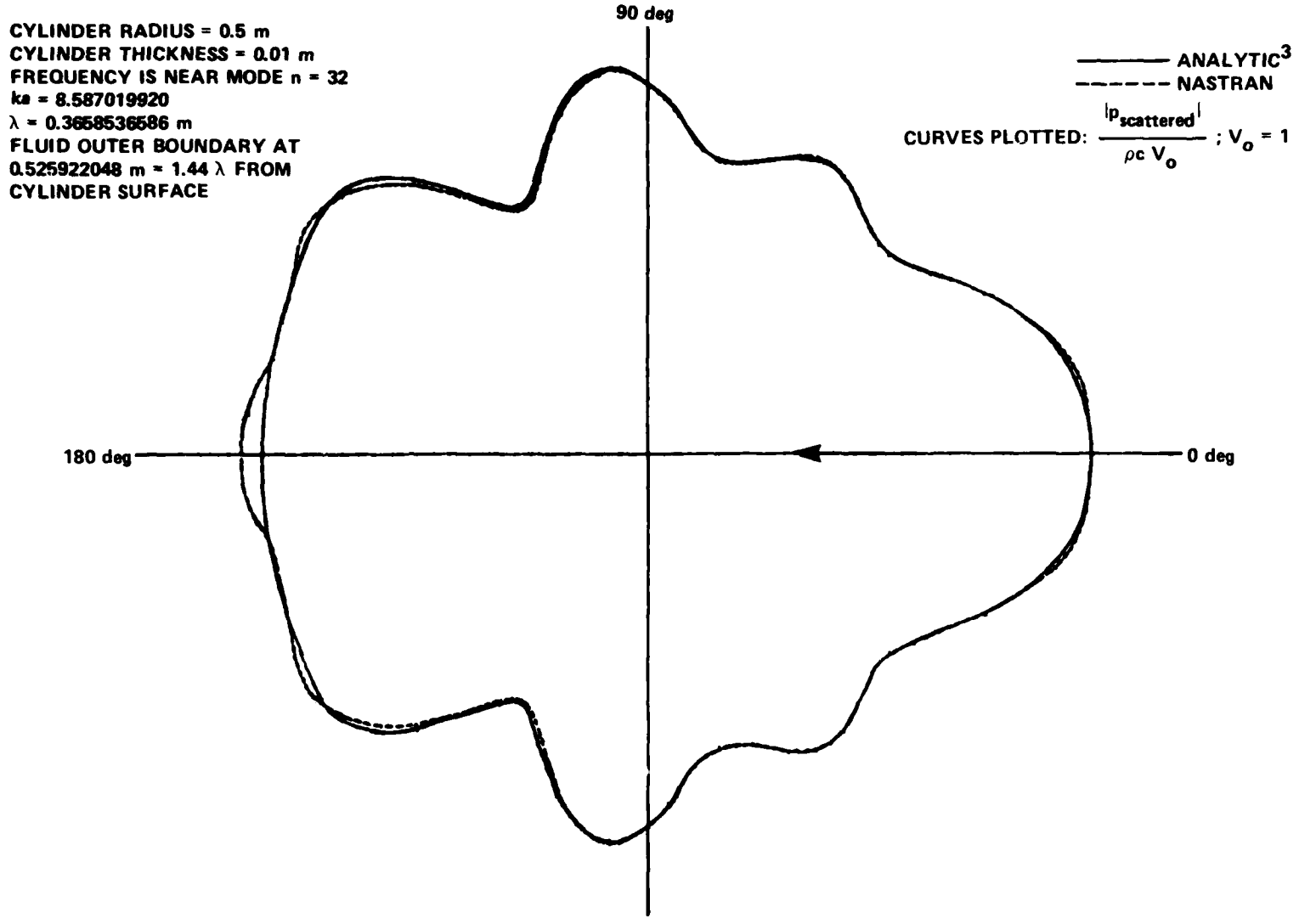

Figure 22 - Calculated Pressures on the Surface of a Cylinder for 4100 Hertz Elastic Scattering

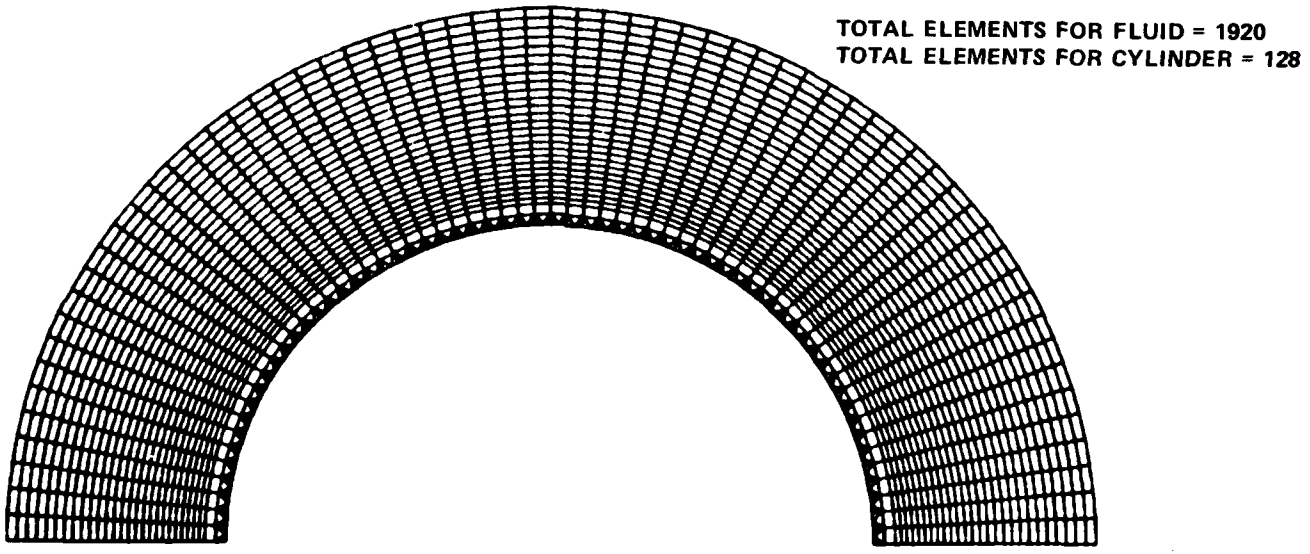

Figure 23 - Finite-Element Mesh for 6600 Hertz Elastic Scattering Calculation

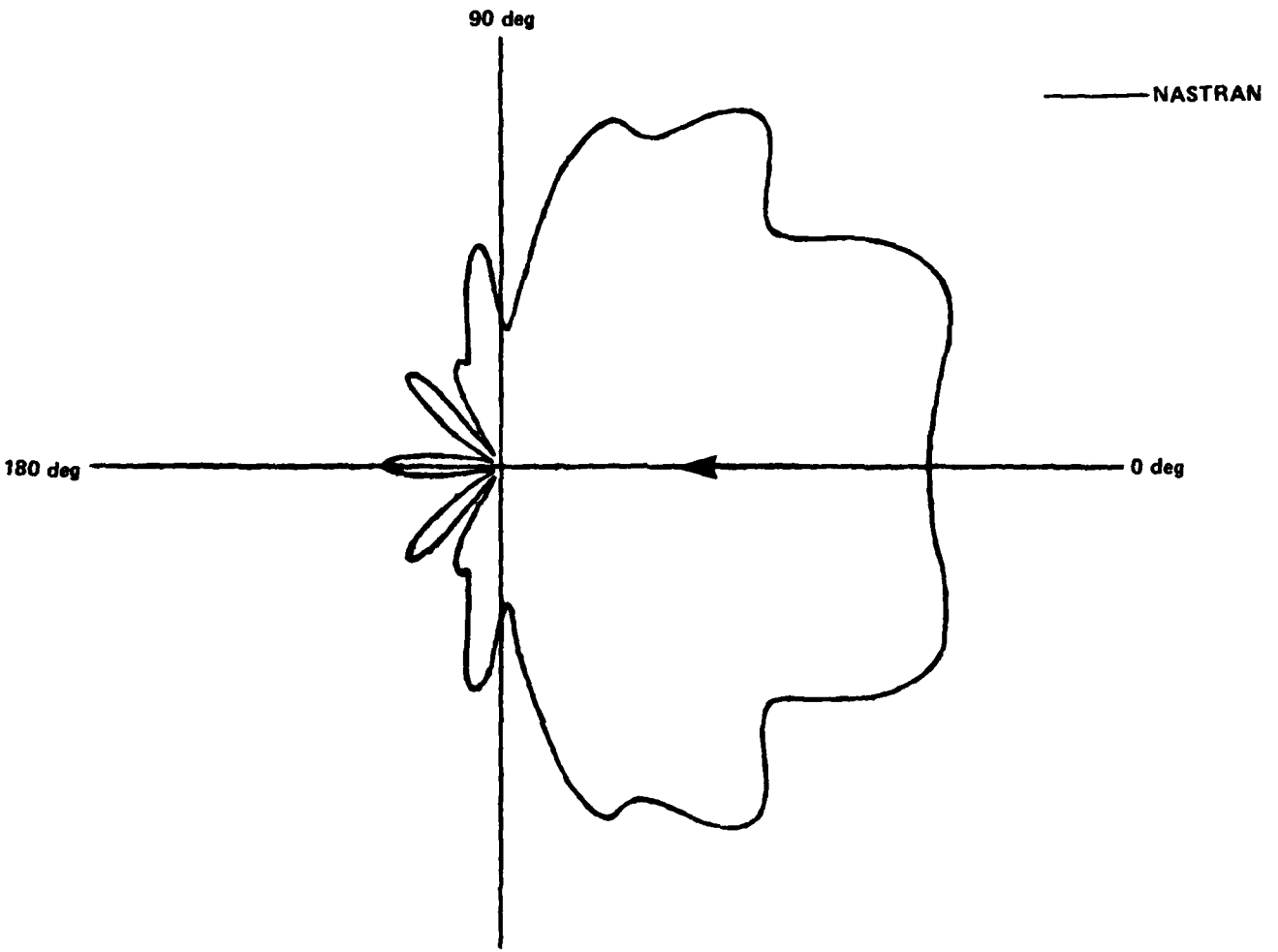

Figure 24 - Calculated Velocities on the Surface of a Cylinder for 6600 Hertz Elastic Scattering

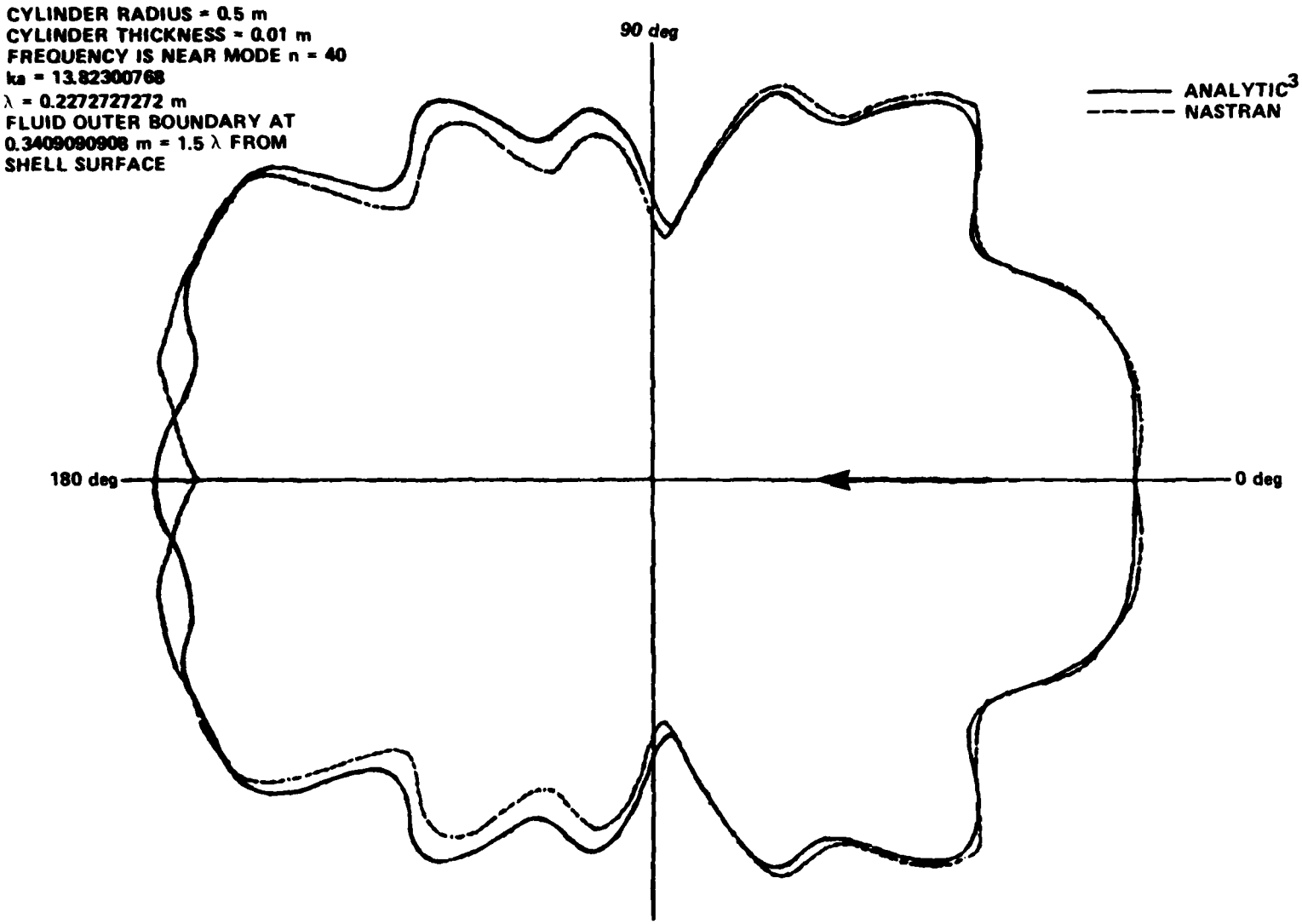

Figure 25 - Calculated Pressures on the Surface of a Cylinder for 6600 Hertz Elastic Scattering

those obtained from several refinements of an initial fluid-structure mesh, three in the first case, two in the second, and one in the last.

Although generally very good convergence to analytic results was obtained for 2100 Hz and 4100 Hz, the numerical solution at 6600 Hz shows less tendency toward overall agreement. The region of most significant disagreement is specifically confined to the un-illumined surface. Relative error incurred in the surface pressures in this region ranged to 14.2 percent. Several factors may have contributed to this deterioration in accuracy. One possible factor is the closeness of the wave absorbing boundary to the cylindrical surface, 0.34 m in this case. According to Kalinowski,[4] plane wave absorption cannot be used when the largest dimension of the absorbing boundary is only slightly larger than the corresponding dimension of the body enclosed. Although the diameter of the absorbing boundary (1.6 m) would seem to be more than slightly larger than the cylinder diameter (1 m), the solution may still be subject, because of the closeness, to effects of reflected residuals of the outgoing waves that are not absorbed. Another possible factor is the way the finite-element mesh for the cylinder was set up. For the 6600-Hz run, the initial subdivisioning of the cylinder was not done according to the strategy outlined on page 30. The intent of this run was, rather, to determine whether an adequate mesh at the higher frequency could be obtained by first "squashing" inward the initial mesh for 4100 Hz until the outer boundary was 1.5 wavelengths of the higher frequency, and then, using the squashed-down initial mesh, refining to the total number of fluid elements which gave the 4100-Hz results (Figure 22). Thus, the shell model at 6600 Hz had the same number of elements (128) as it did at 4100 Hz. The original modeling strategy, on the other hand, would have suggested that it have $(40/2 \times 8) = 160$ elements as the beginning base. The rather sharp increase in complexity of the normal surface velocity profile in the region 90-270 deg (Figures 21 and 24) indicates that at 6600 Hz the shell was somewhat undermodeled.

SCATTERING FROM SUBMERGED CONCENTRIC AND ECCENTRIC CYLINDER SYSTEMS WITH CONTAINED FLUID

Figure 26 sketches the physical problem being considered. When the analog formulation is extended to this type of application, it is useful to summarize the physics[3] involved. With fluid inside the outer cylinder, flexing of the cylinder wall in response to the excitation wave initiates pressure waves which propagate

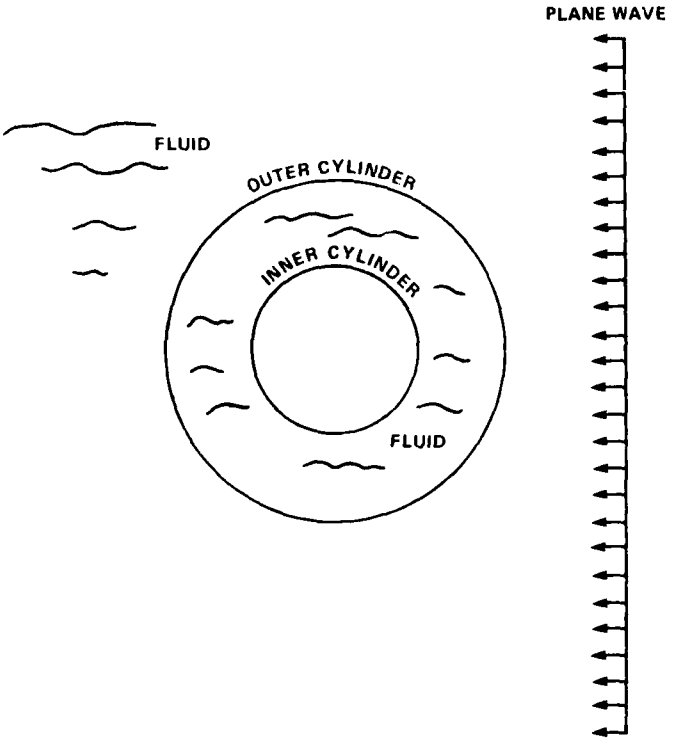

Figure 26 - Submerged Concentric Cylinders with Contained Fluid Ensonified by Plane Wave

inward until they encounter the inner cylinder wall, which in turn sends scattered waves back. In other words, flexing of the outer and inner cylinders results in two pressure wave trains in the enclosed fluid, one travelling inward, the other travelling outward from the center. The two waves combine at any point in the interior fluid to give the <u>total pressure</u>. In particular this pressure, designated $p_{interior}$, exists at the juncture of cylinder wall and fluid.

The analog formulation for exterior scattering is augmented to account for the presence of inner fluid and inner cylinder by (1) incorporating the equations of motion of the inner fluid, (2) accounting for the interior fluid pressure against the cylinder, and (3) including the two boundary conditions on the inner fluid. The first step is accomplished by modeling the interior fluid with finite elements. The second step is accomplished by noting that the force of a positive interior pressure at the cylinder, has the opposite sign from the force of a positive exterior

scattered pressure. Hence the total forces acting at a shell grid point are (see Equation (35))

$$\underset{\sim}{F}_1 = - \underset{\sim\sim}{Ap}_i - \underset{\sim\sim}{Ap}_{se} + \underset{\sim\sim}{Ap}_{interior} \tag{50}$$

Since $p_{interior}$ is unknown, the third term joins the second in moving to the left-hand side of an augmented Equation (31), and the right-hand side (Equation (45)) remains as before. Lastly, boundary conditions on the fluid are considered. The outer boundary condition is

$$\frac{\partial p_{interior}}{\partial n} = - \rho \ddot{U}_n \tag{51}$$

which as before (page 22) is obtained by specifying a force

$$\underset{\sim}{F}_3 = - \mu_e \underset{\sim}{A\rho} \ddot{\underset{\sim}{U}}_n = - \underset{\sim}{A\rho} \ddot{\underset{\sim}{U}}_n \tag{52}$$

which, under the transformation required for symmetry, yields

$$\underset{\sim}{g}_3 = - \frac{1}{\rho} \int_o^t \underset{\sim}{F}_3 \, dt = \underset{\sim}{A} \dot{\underset{\sim}{U}}_n \tag{53}$$

In the same manner the force on the inner boundary is

$$\underset{\sim}{F}_{\substack{\text{inner} \\ \text{boundary}}} = - \underset{\sim}{A}_{\substack{\text{inner} \\ \text{boundary}}} \rho \ddot{\underset{\sim}{w}}_n \tag{54}$$

where w denotes radial displacement of the inner cylinder surface (or, equivalently, the adjacent fluid particles since continuity is assumed) and thus

$$\underset{\sim}{g}_{\substack{\text{inner} \\ \text{boundary}}} = \underset{\sim}{A}_{\substack{\text{inner} \\ \text{boundary}}} \dot{\underset{\sim}{w}}_n \tag{55}$$

For the computations made here, the inner cylinder was assumed to be rigid, so that $g_{inner\ boundary} = 0$ because total velocity is zero at a rigid surface, making no contribution to g_3.

The introduction of interior fluid and structure results in an augmented version of Equation (31)

$$\begin{bmatrix} M & 0 & 0 \\ 0 & -Q_e/\rho & 0 \\ 0 & 0 & -Q_i/\rho \end{bmatrix} \begin{Bmatrix} \ddot{U} \\ \ddot{q}_e \\ \ddot{q}_i \end{Bmatrix} + \begin{bmatrix} B & A & -A \\ A^T & -C_e/\rho & 0 \\ -A^T & 0 & -C_i/\rho \end{bmatrix} \begin{Bmatrix} \dot{U} \\ \dot{q}_e \\ \dot{q}_i \end{Bmatrix}$$

$$+ \begin{bmatrix} K & 0 & 0 \\ 0 & -H_e/\rho & 0 \\ 0 & 0 & -H_i/\rho \end{bmatrix} \begin{Bmatrix} U \\ q_e \\ q_i \end{Bmatrix} = \begin{Bmatrix} f_1 \\ g_2 \\ 0 \end{Bmatrix} \qquad (56)$$

in which subscripts i and e denote interior and exterior, respectively, and $\dot{q}_i = p_{interior}$.

To implement this formulation, the interface between the cylindrical shell and adjacent fluids is modeled as shown in Figure 27. The shell interface with the interior fluid is handled in the same manner as that with the exterior fluid. A new set of grid points is introduced to represent the interface boundary of the interior fluid, these points being coincident with the respective shell grid points, and zero-valued spring connections are used as before to aid the resequencing algorithm (see page 25). Because of the spatial coincidence of the shell grid points with adjacent exterior and interior fluid grid points, the surface area (Figure 6) assigned each structural grid point is also assigned to its neighboring fluid grid points. Area components of the coupling partitions (A^T,A,$-A^T$,-A) of the damping matrix in Equation (56) are inserted, as before, with "DMIG" cards (see page 26), taking care that areas associated with the inner fluid coupling are given a negative sign.

Calculations were made for two cases: 1) the interior cylinder concentric with the outer one, and 2) the interior cylinder offset from the center of the outer one.

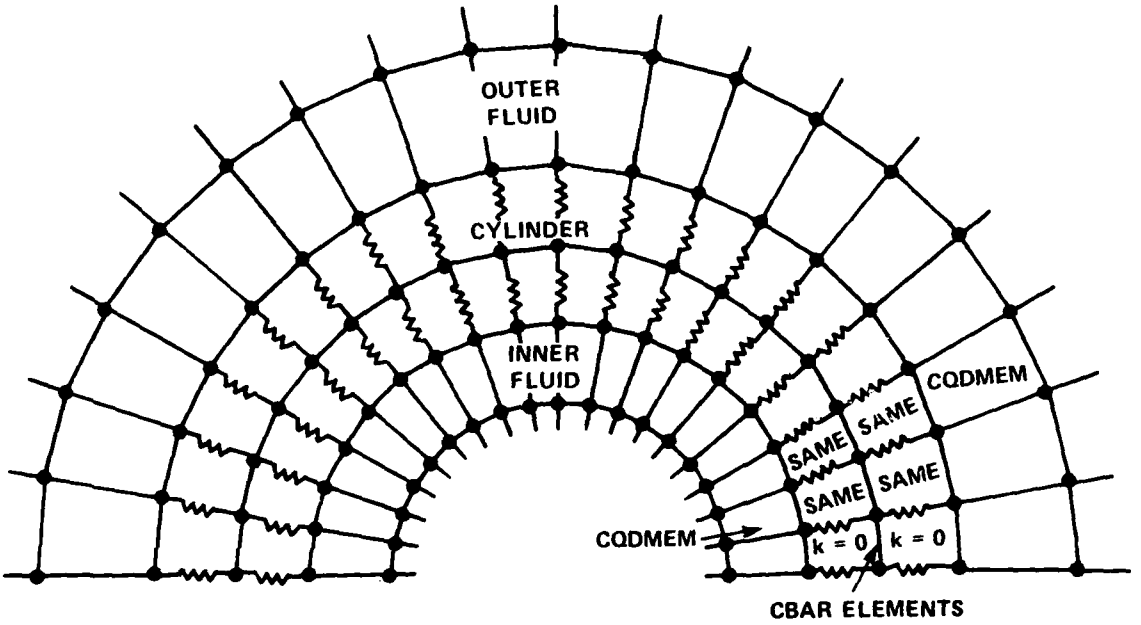

Figure 27 - Finite-Element Model of Cylindrical Shell Interface with Exterior and Interior Fluids

Since at the time of calculation no analytic or other results were at hand for checking, efforts were made to build into the model some level of confidence from results achieved in previous runs. To this end, the exterior fluid and structural model from the 2100 Hertz calculation (Figure 17) was used again for the outer fluid, and the interior fluid was modeled with a mesh of somewhat higher density than that of the outer fluid. The combined total mesh is shown in Figure 28. Figure 29 compares scattered pressures calculated on the surface of the outer cylinder with the previous results (Figure 19) for the same cylinder when it was empty.

For the second calculation, the interior cylinder was shifted 0.03 m from the center of the outer circle. Figure 30 shows the mesh for this run and Figure 31 compares the results with the concentric case.

These two calculations suggest one of the major benefits from the method of structural analogies: the method may permit one to take advantage of the considerable versatility and variety of application inherent in some of the general purpose structural analysis programs available for solving finite element formulations.

OUTER CYLINDER RADIUS = 0.5 m
INNER CYLINDER RADIUS = 0.254 m

TOTAL ELEMENTS FOR EXTERIOR FLUID = 792
TOTAL ELEMENTS FOR INTERIOR FLUID = 528
TOTAL ELEMENTS FOR OUTER ELASTIC CYLINDER = 96

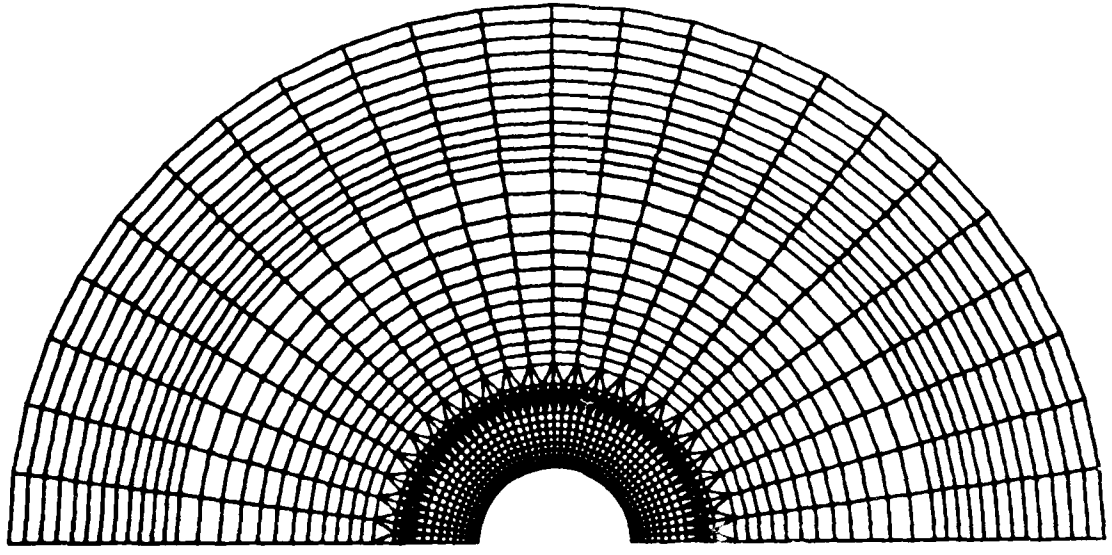

Figure 28 - Finite-Element Mesh for Submerged Elastic Cylinder Enclosing Fluid Bounded by a Rigid Concentric Cylinder, Frequency = 2100 Hertz

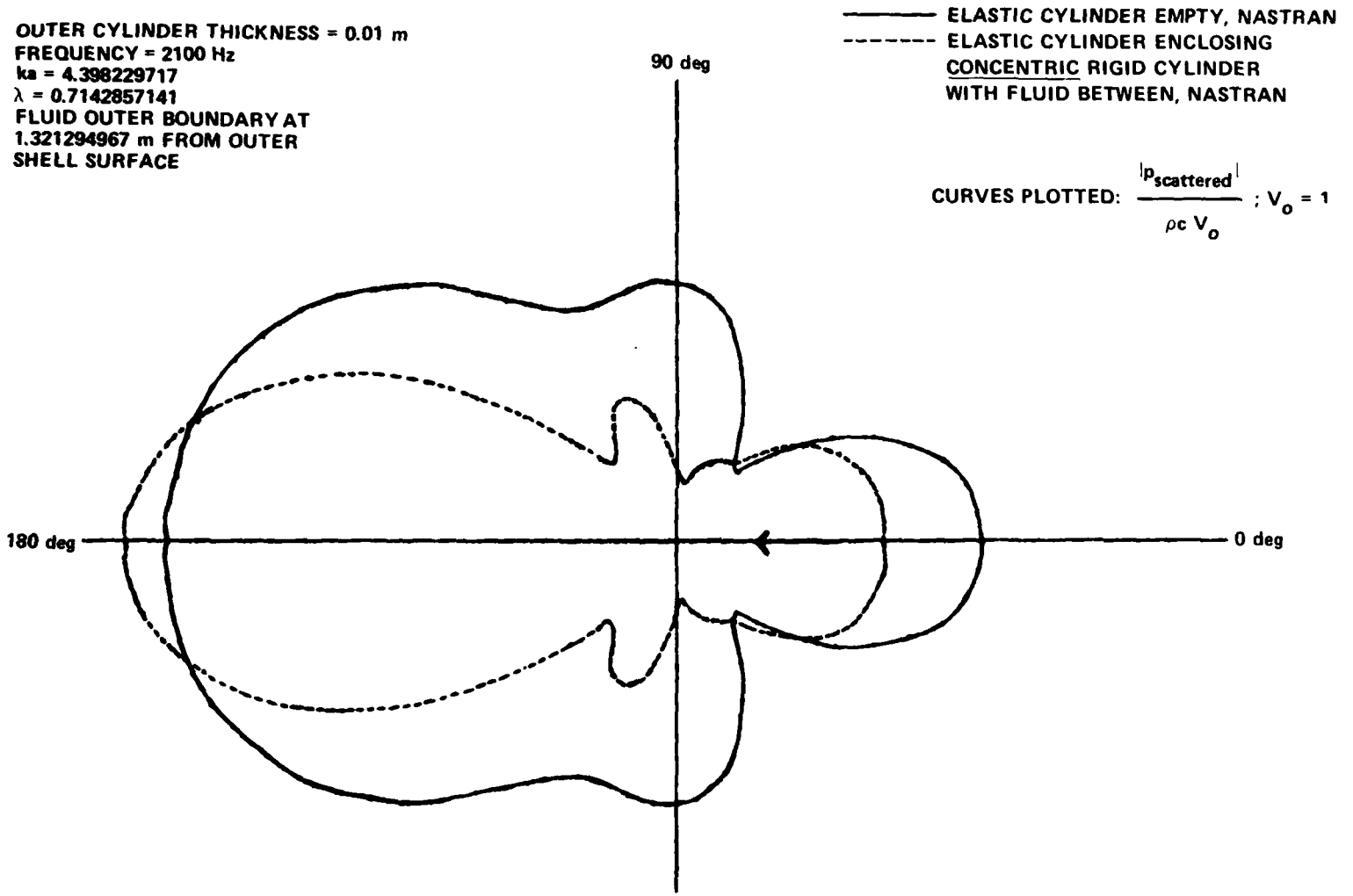

Figure 29 - Comparison of Pressures Scattered by an Empty Cylinder with Pressures Scattered When it Contains a Fluid Bounded by a Rigid Concentric Cylinder

OUTER CYLINDER RADIUS = 0.5 m
INNER CYLINDER RADIUS = 0.254 m
INNER CYLINDER OFFSET FROM CENTER = 0.03 m
TOTAL ELEMENTS FOR EXTERIOR FLUID = 792
TOTAL ELEMENTS FOR INTERIOR FLUID = 576
TOTAL ELEMENTS FOR OUTER ELASTIC CYLINDER = 96

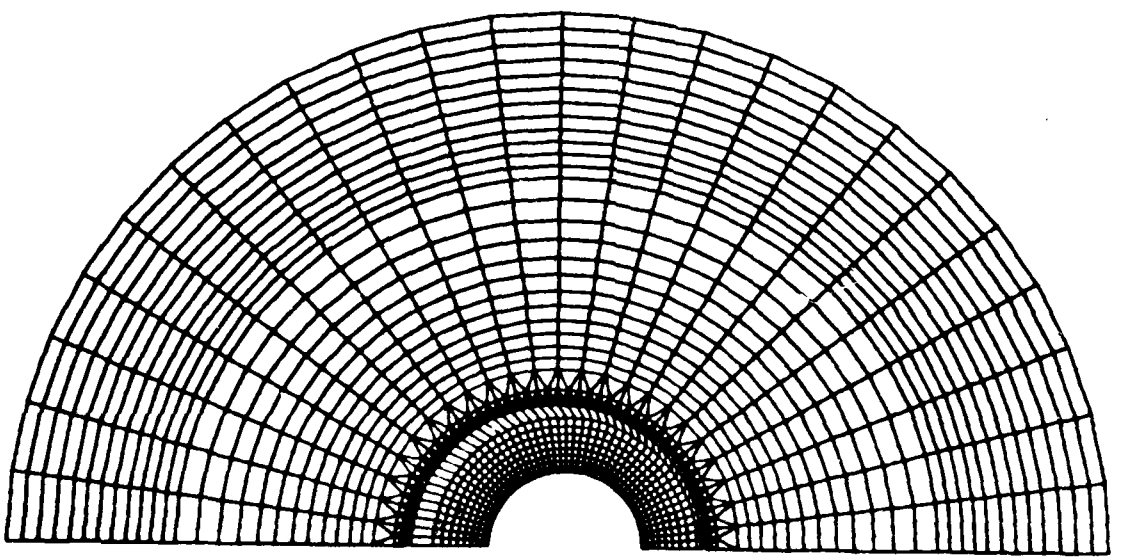

Figure 30 - Finite-Element Mesh for Submerged Elastic Cylinder Enclosing a Fluid Bounded by an Offset Rigid Cylinder, Frequency = 2100 Hertz

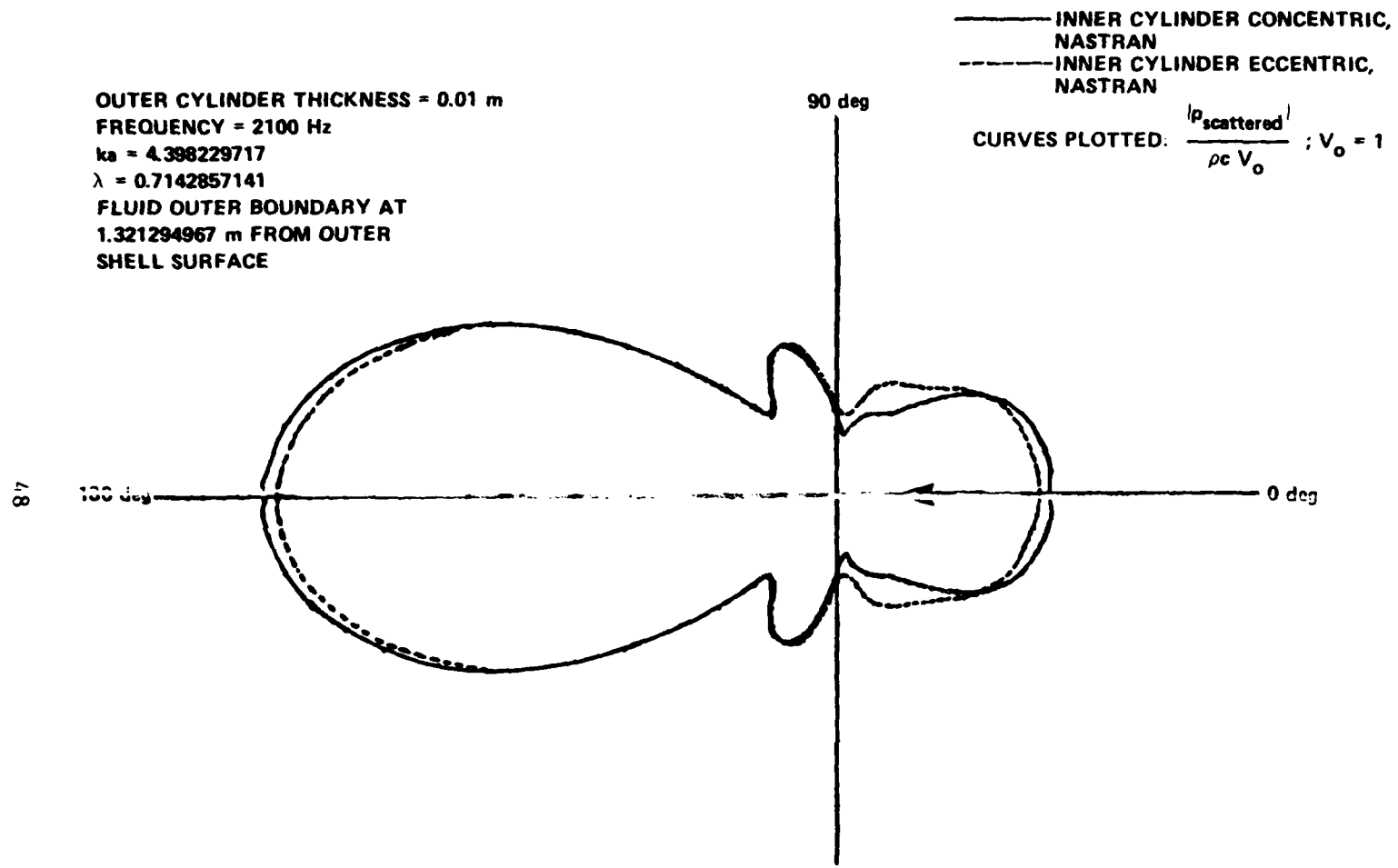

Figure 31 - Effect on Pressure Scattered by a Submerged Elastic Cylinder Enclosing Fluid Bounded by a Rigid Cylinder When the Rigid Cylinder is Offset

SUMMARY

Our experiences in applying a structural analog method to plane-wave 2-D scattering can be summarized as follows:

1. Computations have been made thus for only at frequencies in the lower portions (2kc to ~7kc) of the range (1kc - 20kc) considered relevant to this project.

2. When both structure and fluid were adequately represented in the finite element model, computed structural surface pressures were in excellent agreement with available analytic results.

3. Problem size, which for our applications was governed primarily by the number of finite elements required to model the fluid, increased significantly as frequency increased, despite the fact that the fluid outer boundary moved closer to the structural surface, i.e., less fluid was being modeled.

4. The method, implemented through NASTRAN, is capable of handling applications involving arbitrary structural shapes and structure-fluid configurations.

PROJECTED FUTURE DEVELOPMENT

It is anticipated that future developmental efforts associated with the structural analog approach will be directed toward

1. Assessing performance of plane wave absorption at higher frequencies than have so far been computed.

2. Assessing the merits of a "high frequency" version of the structural analog formulation in which the exterior fluid is discarded from the model.

3. Developing interfaces between computed output from the finite-element model (structural surface pressures and velocities) and algorithms which can use these data to compute pressures at field points outside the finite element model.

4. Increasing our store of analytic and/or experimental results for use in verifying numerical results.

ACKNOWLEDGMENTS

Appreciation is expressed to Gordon C. Everstine and Myles M. Hurwitz for their very generous help and assistance throughout the course of this project.

REFERENCES

1. Wylie, C. R. Jr., "Advanced Engineering Mathematics," McGraw-Hill, New York, London (1960).

2. Everstine, G. C., "Structural Analogies for Scalar Field Problems," International Journal for Numerical Methods in Engineering, 17, pp. 471-476 (1981).

3. Junger, M. C. and D. Fiet, "Sound, Structures and Their Interactions," The MIT Press, Cambridge, Massachusetts (1972).

4. Kalinowski, A. J., "Fluid-Structure Interactions" in "Shock and Vibration Computer Programs, Reviews and Summaries," SVM-10, edited by W. Pilkey and B. Pilkey, The Shock and Vibration Information Center, U.S. Naval Research Laboratory, Washington, D.C., p. 405 (1975).

5. Zienkiewicz, O. C. and R. E. Newton, "Coupled Vibrations of a Structure Submerged in a Compressible Fluid," ISD-ISSC Proceedings on Finite-Element Techniques, University of Stuttgart, Germany (June 1969).

6. McKee, J. M. and M. E. Golden, "GPRIME: A Geometric Language for Finite-Element Modeling, Program Manual," DTNSRDC Report in preparation.

7. Hulbert, L. E. et al., "Structural Analysis via Generalized Interactive Graphics STAGING Volume II," Battelle Columbus Laboratories, Columbus, Ohio (Sep 1979).

8. Everstine, G. C., "A Symmetric Potential Formulation for Fluid-Structure Interaction," Journal of Sound and Vibration, 79(1), 157-160 (8 Nov 1981).

9. Kinsler, E. L. and A. R. Frey, "Fundamentals of Acoustics," Table I, John Wiley & Sons, Inc., New York (1962).

10. Everstine, G. C., "Bandit User's Guide," CMLD Technical Memorandum, TM-184-77-03, Revision B (Dec 1978).

INITIAL DISTRIBUTION

Copies		
1	CHONR	
	1	Code 439/N. Basdekas
2	NAVSEA	
	1	05H/S. Blazek
	1	05H/C. Taylor
12	DTIC	
1	Penn State U ARL/D. Thompson	

CENTER DISTRIBUTION

Copies	Code	Name
1	172	M. A. Krenzke
1	1720.3	R. F. Jones, Jr.
1	18	G. H. Gleissner
1	1802	H. J. Lugt
1	1805	E. H. Cuthill
2	1809.3	D. Harris
1	1824	S. Berkowitz
1	184	J. W. Schot
1	1844	S. K. Dhir
1	1844	G. C. Everstine
1	1844	F. M. Henderson
1	185	T. Corin
1	19	M. Sevik
1	1901	M. Strasberg
1	1902	G. Maidanik
1	1903	G. Chertock
1	1905.2	W. Reader
1	196	D. Feit
1	1962	A. K. Kukk
1	1962	T. Eisler
1	1962	A. Zaloumis
1	1965	M. Rumerman
1	1965	Y. N. Liu
1	274	L. J. Argiro
1	2740	Y. F. Wang
10	5211.1	Reports Distribution
1	522.1	Lib (C)
1	522.2	Lib (A)
1	93	L. Marsh

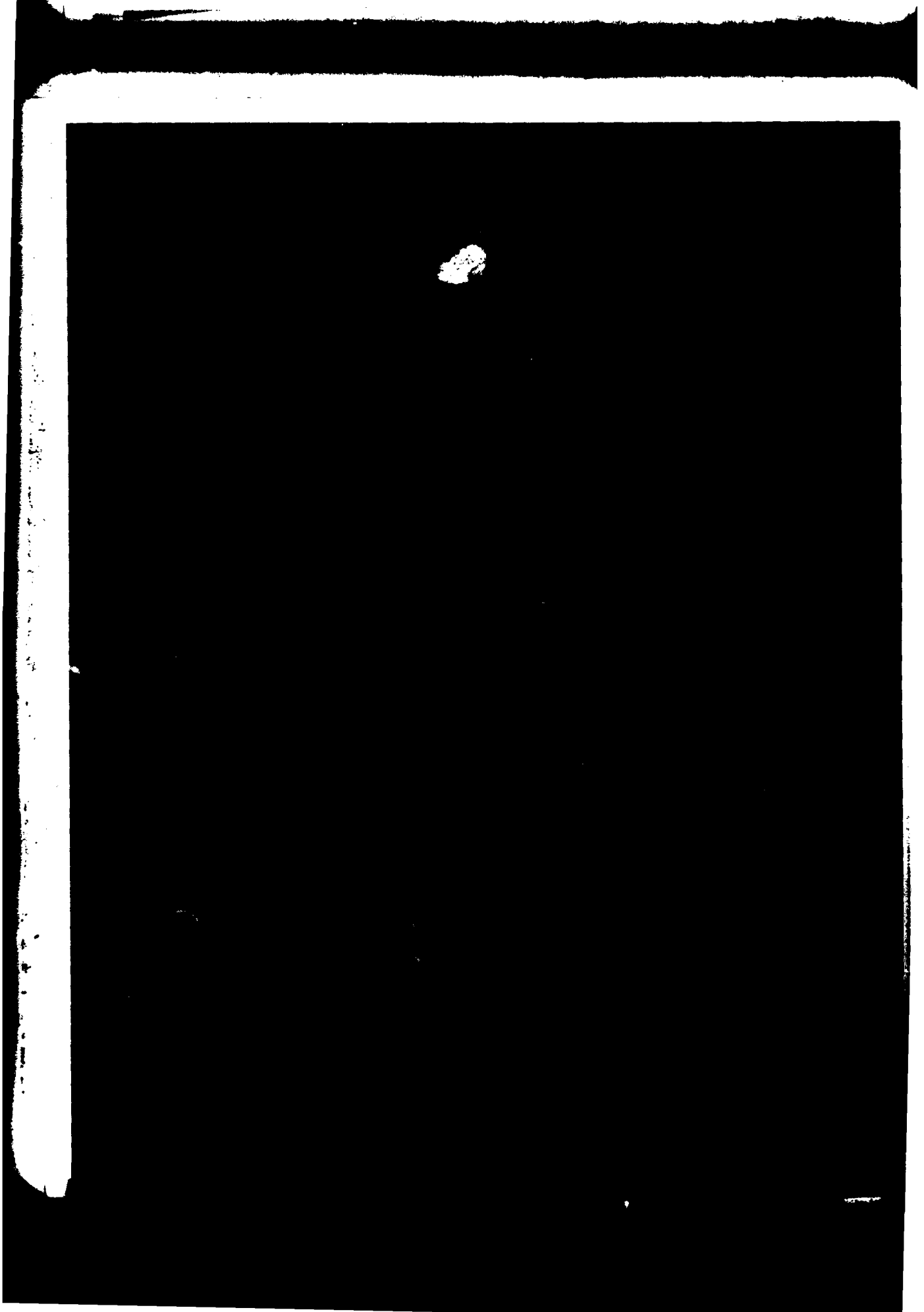


DA
FIL